



Measurement of the CP-violating weak phase ϕ_s and the decay width difference $\Delta\Gamma_s$ using the $B_s^0 \rightarrow J/\psi \phi(1020)$ decay channel in pp collisions at $\sqrt{s} = 8$ TeV

The CMS Collaboration*

Abstract

The CP-violating weak phase ϕ_s of the B_s^0 meson and the decay width difference $\Delta\Gamma_s$ of the B_s^0 light and heavy mass eigenstates are measured with the CMS detector at the LHC using a data sample of $B_s^0 \rightarrow J/\psi \phi(1020) \rightarrow \mu^+ \mu^- K^+ K^-$ decays. The analysed data set corresponds to an integrated luminosity of 19.7 fb^{-1} collected in pp collisions at a centre-of-mass energy of 8 TeV. A total of 49 200 reconstructed B_s^0 decays are used to extract the values of ϕ_s and $\Delta\Gamma_s$ by performing a time-dependent and flavour-tagged angular analysis of the $\mu^+ \mu^- K^+ K^-$ final state. The weak phase is measured to be $\phi_s = -0.075 \pm 0.097$ (stat) ± 0.031 (syst) rad, and the decay width difference is $\Delta\Gamma_s = 0.095 \pm 0.013$ (stat) ± 0.007 (syst) ps^{-1} .

Published in Physics Letters B as doi:10.1016/j.physletb.2016.03.046.

1 Introduction

While no direct evidence of physics beyond the standard model (SM) has yet been found at the CERN LHC, the B_s^0 meson provides a rich source of possibilities to probe its consistency. In this Letter, a measurement of the weak phase ϕ_s of the B_s^0 meson and the decay width difference $\Delta\Gamma_s$ between the light and heavy B_s^0 mass eigenstates is presented, using the data collected by the CMS experiment in pp collisions at the LHC with a centre-of-mass energy of 8 TeV, corresponding to an integrated luminosity of 19.7 fb^{-1} .

The CP-violating weak phase ϕ_s originates from the interference between direct B_s^0 meson decays into a CP eigenstate $c\bar{c}s\bar{s}$ and decays through B_s^0 - \bar{B}_s^0 mixing to the same final state. Neglecting penguin diagram contributions [1][2], ϕ_s is related to the elements of the Cabibbo–Kobayashi–Maskawa quark mixing matrix by $\phi_s \simeq -2\beta_s$, where $\beta_s = \arg(-V_{ts}V_{tb}^*/V_{cs}V_{cb}^*)$. The prediction for $2\beta_s$, determined via a global fit to experimental data within the SM, is $2\beta_s = 0.0363_{-0.0015}^{+0.0016} \text{ rad}$ [3]. Since the value predicted by the SM is very precise, any significant deviation of the measured value from this prediction would be particularly interesting, as it would indicate a possible contribution of new, unknown particles to the loop diagrams describing B_s^0 mixing. The theoretical prediction for the decay width difference $\Delta\Gamma_s$ between the light and heavy B_s^0 mass eigenstates B_L and B_H , assuming no new physics in B_s^0 - \bar{B}_s^0 mixing, is $\Delta\Gamma_s = \Gamma_L - \Gamma_H = 0.087 \pm 0.021 \text{ ps}^{-1}$ [4].

The weak phase ϕ_s was first measured by the Tevatron experiments [5–8], and then at the LHC by the LHCb and ATLAS experiments [9–13], using $B_s^0 \rightarrow J/\psi \phi(1020)$, $B_s^0 \rightarrow J/\psi f_0(980)$, and $B_s^0 \rightarrow J/\psi \pi^+\pi^-$ decays to $\ell^+\ell^-h^+h^-$, where ℓ denotes a muon in the present analysis and h stands for a kaon or a pion. Final states that do not have a single CP eigenvalue require an angular analysis to disentangle the CP-odd and CP-even components. The time-dependent angular analysis can be performed by measuring the decay angles of the final-state particles $\ell^+\ell^-h^+h^-$ and the proper decay time of the B_s^0 multiplied by the speed of light [14], referred to as ct in what follows. In this Letter, the $B_s^0 \rightarrow J/\psi \phi(1020)$ decay to the final state $\mu^+\mu^-K^+K^-$ is analysed, and possible additional contributions to the result from the nonresonant decay $B_s^0 \rightarrow J/\psi K^+K^-$ are taken into account by including a term for an additional amplitude (S -wave) in the fit.

In this measurement the transversity basis is used [14]. The three angles $\Theta = (\theta_T, \psi_T, \varphi_T)$ of the transversity basis are illustrated in Fig. 1. The angles θ_T and φ_T are the polar and azimuthal angles, respectively, of the μ^+ in the rest frame of the J/ψ where the x axis is defined by the direction of the $\phi(1020)$ meson in the J/ψ rest frame, and the x - y plane is defined by the decay plane of the $\phi(1020) \rightarrow K^+K^-$. The helicity angle ψ_T is the angle of the K^+ in the $\phi(1020)$ rest frame with respect to the negative J/ψ momentum direction.

The differential decay rate of $B_s^0 \rightarrow J/\psi \phi(1020)$ is represented using the function $f(\Theta, ct, \alpha)$ as in Ref. [15]:

$$\frac{d^4\Gamma(B_s^0)}{d\Theta d(ct)} = f(\Theta, ct, \alpha) \propto \sum_{i=1}^{10} O_i(ct, \alpha) g_i(\Theta), \quad (1)$$

where O_i are time-dependent functions, g_i are angular functions, and α is a set of physics parameters.

The functions $O_i(ct, \alpha)$ are:

$$O_i(ct, \alpha) = N_i e^{-ct/c\tau} \left[a_i \cosh\left(\frac{\Delta\Gamma_s t}{2}\right) + b_i \sinh\left(\frac{\Delta\Gamma_s t}{2}\right) + c_i \cos(\Delta m_s t) + d_i \sin(\Delta m_s t) \right],$$

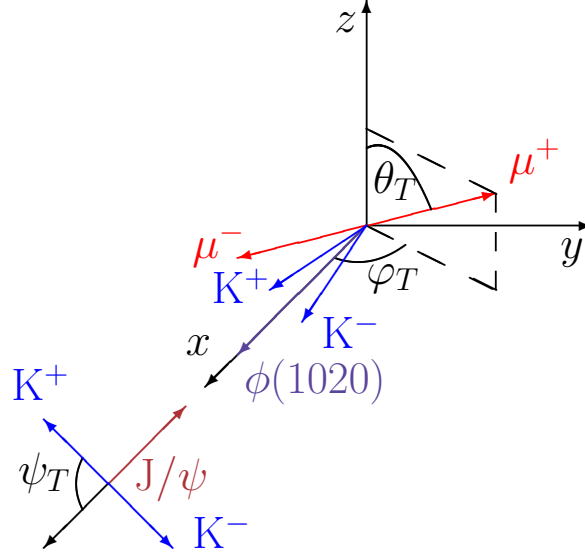


Figure 1: Definition of the three angles θ_T , ψ_T , and φ_T describing the decay topology of $B_s^0 \rightarrow J/\psi \phi(1020)$. See text for details.

where Δm_s is the mass difference between the heavy and light B_s^0 mass eigenstates, $c\tau$ is defined as the product of the lifetime and the speed of light, the function $g_i(\Theta)$ and the terms N_i , a_i , b_i , c_i , and d_i are given in Table 1.

Table 1: Angular and time-dependent terms of the signal model.

i	$g_i(\theta_T, \psi_T, \varphi_T)$	N_i	a_i	b_i	c_i	d_i
1	$2 \cos^2 \psi_T (1 - \sin^2 \theta_T \cos^2 \varphi_T)$	$ A_0(0) ^2$	1	D	C	$-S$
2	$\sin^2 \psi_T (1 - \sin^2 \theta_T \sin^2 \varphi_T)$	$ A_{\parallel}(0) ^2$	1	D	C	$-S$
3	$\sin^2 \psi_T \sin^2 \theta_T$	$ A_{\perp}(0) ^2$	1	$-D$	C	S
4	$-\sin^2 \psi_T \sin 2\theta_T \sin \varphi_T$	$ A_{\parallel}(0) A_{\perp}(0) $	$C \sin(\delta_{\perp} - \delta_{\parallel})$	$S \cos(\delta_{\perp} - \delta_{\parallel})$	$\sin(\delta_{\perp} - \delta_{\parallel})$	$D \cos(\delta_{\perp} - \delta_{\parallel})$
5	$\frac{1}{\sqrt{2}} \sin 2\psi_T \sin^2 \theta_T \sin 2\varphi_T$	$ A_0(0) A_{\parallel}(0) $	$\cos(\delta_{\parallel} - \delta_0)$	$D \cos(\delta_{\parallel} - \delta_0)$	$C \cos(\delta_{\parallel} - \delta_0)$	$-S \cos(\delta_{\parallel} - \delta_0)$
6	$\frac{1}{\sqrt{2}} \sin 2\psi_T \sin 2\theta_T \sin \varphi_T$	$ A_0(0) A_{\perp}(0) $	$C \sin(\delta_{\perp} - \delta_0)$	$S \cos(\delta_{\perp} - \delta_0)$	$\sin(\delta_{\perp} - \delta_0)$	$D \cos(\delta_{\perp} - \delta_0)$
7	$\frac{2}{3}(1 - \sin^2 \theta_T \cos^2 \varphi_T)$	$ A_S(0) ^2$	1	$-D$	C	S
8	$\frac{1}{3}\sqrt{6} \sin \psi_T \sin^2 \theta_T \sin 2\varphi_T$	$ A_S(0) A_{\parallel}(0) $	$C \cos(\delta_{\parallel} - \delta_S)$	$S \sin(\delta_{\parallel} - \delta_S)$	$\cos(\delta_{\parallel} - \delta_S)$	$D \sin(\delta_{\parallel} - \delta_S)$
9	$\frac{1}{3}\sqrt{6} \sin \psi_T \sin 2\theta_T \cos \varphi_T$	$ A_S(0) A_{\perp}(0) $	$\sin(\delta_{\perp} - \delta_S)$	$-D \sin(\delta_{\perp} - \delta_S)$	$C \sin(\delta_{\perp} - \delta_S)$	$S \sin(\delta_{\perp} - \delta_S)$
10	$\frac{4}{3}\sqrt{3} \cos \psi_T (1 - \sin^2 \theta_T \cos^2 \varphi_T)$	$ A_S(0) A_0(0) $	$C \cos(\delta_0 - \delta_S)$	$S \sin(\delta_0 - \delta_S)$	$\cos(\delta_0 - \delta_S)$	$D \sin(\delta_0 - \delta_S)$

The terms C , S , and D are defined as:

$$C = \frac{1 - |\lambda|^2}{1 + |\lambda|^2}, \quad S = -\frac{2|\lambda| \sin \phi_s}{1 + |\lambda|^2}, \quad D = -\frac{2|\lambda| \cos \phi_s}{1 + |\lambda|^2},$$

using the same sign convention as the LHCb experiment [10]. Equation (1) represents the model for B_s^0 . The model for \bar{B}_s^0 is obtained by changing the sign of the c_i and d_i terms. The parameters $|A_{\perp}|^2$, $|A_0|^2$, and $|A_{\parallel}|^2$ are the magnitudes squared of the perpendicular, longitudinal, and parallel P -wave amplitudes, respectively; $|A_S|^2$ is the magnitude squared of the S -wave amplitude representing the fraction of nonresonant decay $B_s^0 \rightarrow J/\psi K^+ K^-$; the parameters δ_{\perp} , δ_0 , δ_{\parallel} , and δ_S are their corresponding strong phases.

The complex parameters λ_f are defined as $\lambda_f = (q/p)(A_f/\bar{A}_f)$, where the amplitudes A_f (\bar{A}_f) describe the decay of a B_s^0 (\bar{B}_s^0) meson to a final state f , and the parameters p and q relate the mass and flavour eigenstates as $B_H = pB_s^0 - q\bar{B}_s^0$ and $B_L = pB_s^0 + q\bar{B}_s^0$ [16]. Assuming polarisation-independent CP-violation effects, λ_f can be simplified as $\lambda_f = \eta_f \lambda$, where η_f is

the CP eigenvalue. The amount of CP violation in mixing is assumed to be negligible [17]. Thus, no $|q/p|$ terms are used in Eq. (1) when going from the B_s^0 model to the \bar{B}_s^0 model. Since direct CP violation is expected to be small theoretically [3] and is measured to be small [9], $|\lambda|$ is set to 1.0.

2 The CMS detector

The central feature of the CMS apparatus is a 13 m long superconducting solenoid of 6 m internal diameter, providing a magnetic field of 3.8 T. Within the solenoid volume are a silicon pixel and strip tracker, a lead tungstate crystal electromagnetic calorimeter, and a brass and scintillator hadron calorimeter, each composed of a barrel and two endcap sections. Muons are measured in gas-ionisation detectors embedded in the steel flux-return yoke outside the solenoid. Extensive forward calorimetry complements the coverage provided by the barrel and endcap detectors.

The main subdetectors used for the present analysis are the silicon tracker and the muon detection system. The silicon tracker measures charged particles within the pseudorapidity range $|\eta| < 2.5$. It consists of 66 million $100 \times 150 \mu\text{m}^2$ silicon pixels and more than 9 million silicon strips. For nonisolated particles of transverse momentum $1 < p_T < 10 \text{ GeV}$ and $|\eta| < 1.4$, the track resolutions are typically 1.5% in p_T and 25–90 (45–150) μm in the transverse (longitudinal) impact parameter [18].

Muons are measured in the pseudorapidity range $|\eta| < 2.4$, with detection planes made using three technologies: drift tubes, cathode strip chambers, and resistive plate chambers. The relative p_T resolution for low transverse momentum muons with $p_T < 10 \text{ GeV}$ is between 0.8% and 3.0% depending on $|\eta|$ [19].

The first level (L1) of the CMS trigger system, composed of custom hardware processors, uses information from the calorimeters and muon detectors to select the most interesting events in a fixed time interval of less than 4 μs . The high-level trigger (HLT) processor farm further reduces the event rate from around 100 kHz to around 400 Hz, before data storage. At the HLT stage there is full access to all the event information, including tracking, and therefore selections similar to those applied offline can be used.

A more detailed description of the CMS detector, together with a definition of the coordinate system used and the relevant kinematic variables, can be found in Ref. [20].

3 Event selection and simulated samples

A trigger optimised for the detection of B hadrons decaying to J/ψ is used to collect the data sample. The L1 trigger used in this analysis requires two muons, each with p_T greater than 3 GeV and $|\eta| < 2.1$. The HLT requires a J/ψ candidate displaced from the luminous region. Each muon p_T is required to be at least 4 GeV and the p_T of the reconstructed muon pair must be greater than 6.9 GeV. The J/ψ candidates are reconstructed from the muon pairs selected by the trigger in the invariant mass window 2.9–3.3 GeV. The three-dimensional (3D) distance of closest approach of the two muons to each other is required to be smaller than 0.5 cm. The two muon trajectories are fitted to a common decay vertex. The transverse decay length significance $L_{xy}/\sigma_{L_{xy}}$ is required to be greater than 3, where L_{xy} is the distance between the centre of the luminous region and the secondary vertex in the transverse plane, and $\sigma_{L_{xy}}$ is the L_{xy} uncertainty. The secondary-vertex fit probability, calculated using the χ^2 and the number of degrees of freedom of the vertex fit, must be greater than 10%. The angle ρ between the dimuon transverse

momentum and the L_{xy} direction is required to satisfy $\cos \rho > 0.9$.

Offline selection criteria are applied to the sample. The individual muon candidates are required to lie within a kinematic acceptance region of $p_T > 4 \text{ GeV}$ and $|\eta| < 2.1$. Two oppositely charged muon candidates are paired and required to originate from a common vertex. Dimuon candidates with invariant mass within 150 MeV of the world-average J/ψ mass [21] are selected. Candidate $\phi(1020)$ mesons are reconstructed from pairs of oppositely charged tracks with $p_T > 0.7 \text{ GeV}$, after removing the muon candidate tracks forming the J/ψ . Each selected track is assumed to be a kaon, and the invariant mass of a track pair is required to be within 10 MeV of the world-average $\phi(1020)$ mass [21].

The B_s^0 candidates are formed by combining J/ψ and $\phi(1020)$ candidates. A kinematic fit of the two muon and two kaon candidates is performed, with a common vertex, and the dimuon invariant mass is constrained to the nominal J/ψ mass [21]. A B_s^0 candidate is retained if the $J/\psi \phi(1020)$ pair has an invariant mass between 5.20 and 5.65 GeV and the χ^2 vertex fit probability is greater than 2%.

Multiple pp collisions can occur in the same beam crossing (pileup). The average number of primary vertices in an event is approximately 16, and each selected event is required to have at least one reconstructed primary vertex. If there are multiple vertices, the one that minimises the angle between the flight direction and the momentum of the B_s^0 is selected. The selected primary vertex is used to measure ct . The quantity ct is calculated from the transverse decay length vector of the B_s^0 , $\vec{L}_{xy}^{B_s^0}$, as $ct = m_{\text{PDG}}^{B_s^0} \vec{L}_{xy}^{B_s^0} \cdot \vec{p}_T / p_T^2$, where $m_{\text{PDG}}^{B_s^0}$ is the world-average B_s^0 mass [21] and \vec{p}_T is the B_s^0 transverse momentum vector. The decay length is calculated in the transverse plane to minimise effects due to pileup.

Simulated events are produced using the PYTHIA v6.424 Monte Carlo event generator [22]. The B hadron decays are modelled with the EVTGEN simulation package [23]. For the B_s^0 signal generation, the EVTPVVCPLH module is used, which simulates the double vector decay taking into account neutral meson mixing and CP-violating time-dependent asymmetries. Final-state radiation is included in EVTGEN through the PHOTOS package [24, 25]. The events are then passed through a detailed GEANT4-based simulation [26] of the CMS detector. The predicted distributions from simulation of many kinematic and geometric variables are compared to those from data and found to be in agreement. The simulated samples are used to determine the signal reconstruction efficiencies, and to study the background components in the B_s^0 signal mass window.

The main background for the $B_s^0 \rightarrow J/\psi \phi(1020)$ decays originates from nonprompt J/ψ mesons from the decay of B hadrons, such as B^0 , B^\pm , Λ_b , and B_c . Since the B_c cross section is small [21] compared to that of the B_s^0 [21], the B_c decays can be neglected. The contribution of the $\Lambda_b \rightarrow J/\psi X$ channels to the selected events is also found to be small, and its mass distribution in the selected mass range is observed to be flat. The effect of background with a similar signal signature on the physics observables is studied using simulated events, and found to be negligible. The mass distribution in the signal region is shown in Fig. 2, and the distribution of ct and its uncertainty σ_{ct} in Fig. 3.

Efficiency corrections owing to the detector acceptance, trigger selection, and selection criteria applied in the data analysis are taken into account in the modelling of the angular observables. The angular efficiency $\epsilon(\Theta)$ is calculated using a fully simulated sample of $B_s^0 \rightarrow J/\psi \phi(1020) \rightarrow \mu^+ \mu^- K^+ K^-$ decays. In this sample, the $\Delta\Gamma_s$ parameter is set to zero to avoid correlations between the decay time and the angular variables. The $\epsilon(\Theta)$ is fitted to a 3D function of Θ to properly account for the correlation among the angular observables.

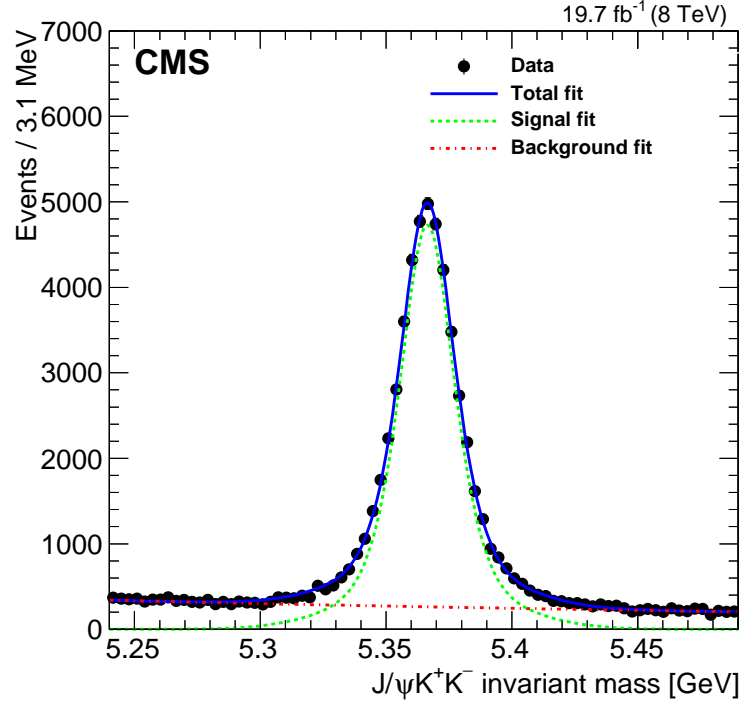


Figure 2: The $J/\psi K^+ K^-$ invariant mass distribution of the B_s^0 candidates. The solid line is a fit to the data (solid markers), the dashed line is the signal component and the dot-dashed line is the background component.

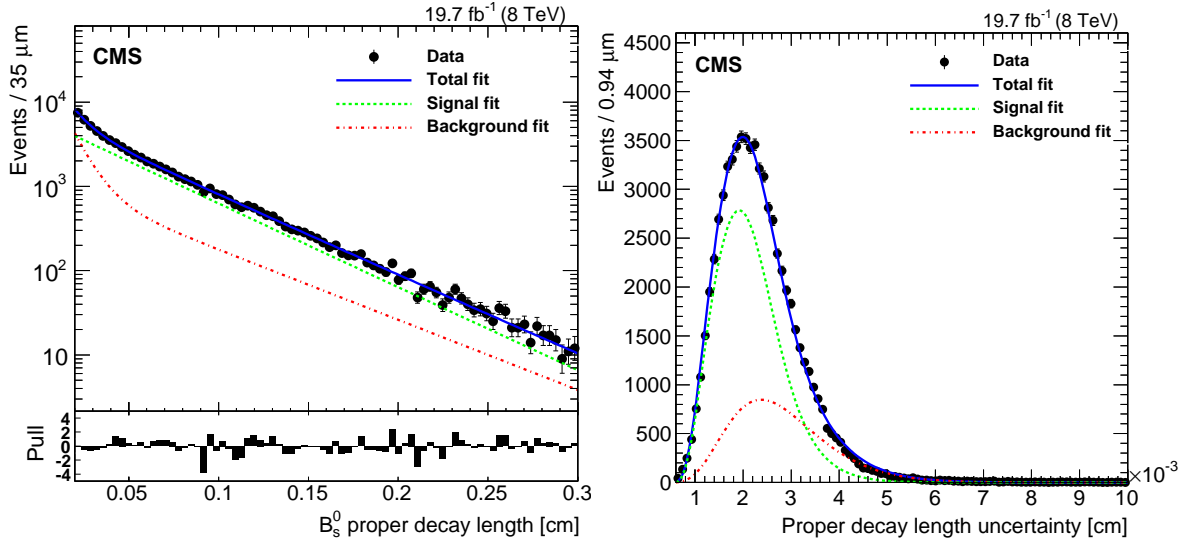


Figure 3: The ct distribution (left) and its uncertainty σ_{ct} (right) of the B_s^0 candidates. The solid line is a fit to the data (solid markers), the dashed line is the signal component and the dot-dashed line is the background component. For the ct distribution the pull, defined as the difference between the observed events and the fit function applied to the sum of the signal and background, divided by the statistical uncertainty in the observed events, is displayed in the histogram in the lower panel.

The trigger includes a decay length significance requirement for the J/ψ candidates. Accordingly, the value of ct is required to be greater than $200 \mu\text{m}$ in order to avoid a lifetime bias coming from the turn-on curve of the trigger efficiency. The efficiency histogram of ct is then fitted with a straight line plus a sigmoid function.

4 Flavour tagging

The flavour of each B_s^0 candidate at production time is determined with an opposite-side (OS) flavour tagging algorithm. Since b quarks are produced as $b\bar{b}$ pairs, the flavour of the signal B_s^0 meson at production time can be inferred from the flavour of the other B hadron in the event. The tagging algorithm used in this analysis requires an additional muon or electron in the events containing a reconstructed $B_s^0 \rightarrow J/\psi \phi(1020)$ decay. The additional lepton is assumed to originate from a semileptonic decay of the OS B hadron, $b \rightarrow \ell \nu X$ decay, with $\ell = e, \mu$. For all the events in which an OS tag lepton is found the algorithm provides a tag decision ζ based on the charge of the lepton: $\zeta = +1$ for signal B_s^0 , and $\zeta = -1$ for signal \bar{B}_s^0 .

The tag decision is affected by processes that reverse the charge-flavour correlation, such as cascade decays $b \rightarrow c \rightarrow \ell$, or semileptonic decays of neutral OS B mesons that have oscillated to their antiparticles before decaying. Leptons produced from flavour-uncorrelated sources, such as semileptonic decays of promptly produced charmed hadrons, pion and kaon decays, J/ψ decays, and Dalitz decays of neutral pions further contribute to diluting the tag information. The probability of assigning a wrong flavour to the signal B_s^0 is described by the mistag probability ω , defined as the ratio of the number of wrongly tagged events divided by the total number of tagged events, which is directly related to the dilution factor $D = (1 - 2\omega)$. The value of ω is estimated from data on a per-event basis, as described below.

The tagging algorithm is optimised by maximising the tagging power $\mathcal{P}_{\text{tag}} = \varepsilon_{\text{tag}}(1 - 2\omega)^2$, which represents the equivalent efficiency of a sample with perfect tagging ($\omega = 0$). The term ε_{tag} is the tagging efficiency, defined as the fraction of events to which a tag decision is found by the tagging algorithm.

Opposite-side muons and electrons are reconstructed with the particle-flow algorithm [27, 28]. In each event, the muons (electrons) that are not part of the reconstructed $B_s^0 \rightarrow J/\psi \phi(1020)$ decay are required to be identified with loose identification criteria. If there are multiple muons (electrons) in the event, the one with the highest p_T is chosen at this stage. The tag lepton selections are then optimised separately for muons and electrons using simulated signal samples of $B_s^0 \rightarrow J/\psi \phi(1020)$ decays. A cut-based opposite-side lepton selection is applied to reduce the number of leptons not originating from B-hadron decays. To optimise the selection, several variables are studied, and a set of five discriminating variables (p_T , η , d_{xyz} , ΔR , Isolation) is identified. A total number of more than four million alternative cut configurations have been tested to determine the configuration that maximises the tagging power, independently for muons and electrons. The tag muon is thus required to have $p_T > 2.2 \text{ GeV}$, the 3D impact parameter d_{xyz} with respect to the primary vertex associated with the signal B_s^0 is required to be smaller than 0.1 cm, and the angular separation, $\Delta R = \sqrt{(\Delta\phi)^2 + (\Delta\eta)^2}$, between the muon and the signal B_s^0 is required to be greater than 0.3, where $\Delta\phi$ and $\Delta\eta$ are the azimuthal angle and pseudorapidity differences between the directions of the tag muon and the B_s^0 candidate. Electrons are required to have $p_T > 2.0 \text{ GeV}$, $d_{xyz} < 0.1 \text{ cm}$, and $\Delta R > 0.2$. In addition, a multivariate discriminator ($\text{MVA}_{e-\pi}$) tuned to separate genuine electrons reconstructed by the particle-flow algorithm from pions and photons is applied to tag electrons by requiring that the discriminator is greater than 0.2 [28].

A multilayer perceptron neural network (MLP-NN) of the TMVA toolkit [29] is used to further separate the right- and wrong-tag leptons. Training and testing is performed using approximately 24 000 and 20 400 simulated $B_s^0 \rightarrow J/\psi \phi(1020)$ events for the muon and electron MLP-NNs, respectively, and two independently optimised sets of variables. Half of each sample is used for training and the other half for testing. The input variables common to both

MLP-NNs are p_T , η , and d_{xyz} of the tag lepton, and two variables related to activity in a cone around the lepton direction: a particle-flow relative isolation variable [28] and a p_T -weighted average of the charges of the particles in the cone. Specific variables are further introduced in the MLP-NNs separately for muons and electrons. For muons, the p_T relative to the axis of the jet containing the muon is used, while for electrons the $MVA_{e-\pi}$ is exploited.

The mistag probabilities are obtained from data using the self-tagging channel $B^\pm \rightarrow J/\psi K^\pm$, where the charge of the reconstructed kaon determines the flavour of the B^\pm and, in the absence of mixing, of the opposite-side B hadron as well. The mistag probabilities are parametrised separately for muons and electrons with analytic functions of the MLP-NN discriminators in order to provide a per-event value of the predicted mistag probability ω . The functional forms of the parametrisations are obtained from the simulated B_s^0 sample. The candidate B^\pm mesons are required to pass a selection as similar as possible to that applied for the reconstruction of the signal B_s^0 candidates. The same trigger and J/ψ reconstruction requirements as for the B_s^0 signal sample are applied. A charged particle with $p_T > 2 \text{ GeV}$, assumed to be a kaon, is combined with the dimuon pair in a kinematic fit. An unbinned extended maximum-likelihood fit to the invariant $J/\psi K^\pm$ mass is performed, yielding a total of $(707 \pm 2) \times 10^3$ reconstructed $B^\pm \rightarrow J/\psi K^\pm$ events. The tagging efficiency evaluated with the $B^\pm \rightarrow J/\psi K^\pm$ data sample is $(4.56 \pm 0.02)\%$ and $(3.92 \pm 0.02)\%$ for muons and electrons, respectively, where the uncertainties are statistical.

The mistag parametrisation curves evaluated with the B^\pm control channel for muons and electrons are shown in Fig. 4, where the parametrisations for the B^\pm and B_s^0 simulated samples are shown for comparison.

Most tagged events have only a single electron or muon tag. If both tags are available for a specific event (about 3.5% of the cases), the tag lepton with the greatest value of the dilution factor is retained, and the tag decision and the estimated mistag are taken from this tag lepton. The overall lepton tagging efficiency is $(8.31 \pm 0.03)\%$, as measured in data with the $B^\pm \rightarrow J/\psi K^\pm$ data sample.

To correct for potential effects induced by the dependence of the tagging algorithm on the $B_s^0 \rightarrow J/\psi \phi(1020)$ simulation, the mistag probability is calibrated by comparing the per-event predicted ω to the measured ω^{meas} obtained from the $B^\pm \rightarrow J/\psi K^\pm$ data control channel. This is then fit to the function $\omega^{\text{meas}} = p_0 + p_1(\omega - \omega')$, chosen to limit the correlation between the function parameters p_0 and p_1 . The parameter ω' is fixed to a value roughly corresponding to the mean of the calculated mistag probability, $\omega' = 0.35$. The resulting calibration parameters are $p_0 = 0.348 \pm 0.003$ and $p_1 = 1.01 \pm 0.03$, and their uncertainties are propagated as a statistical uncertainty in the OS tagger.

The systematic uncertainties related to the calibration parameters p_0 and p_1 are dominated by the dependence of these parameters on the flavour of the signal-side B hadron. The uncertainties are estimated from B^\pm data and simulated samples of B_s^0 and B^\pm events. Systematic uncertainties originating from possible variations in the CMS data-taking conditions, the signal B hadron kinematics, the analytic form of the mistag parametrisation functions, and the model used to fit the B^\pm invariant mass distribution are tested and found to be negligible.

The overall tagging power of the OS lepton tagger, measured with a sample of $B^\pm \rightarrow J/\psi K^\pm$ events, is $\mathcal{P}_{\text{tag}} = (1.307 \pm 0.031 \text{ (stat)} \pm 0.007 \text{ (syst)}) \%$, corresponding to the combined mistag probability $\omega = (30.17 \pm 0.24 \text{ (stat)} \pm 0.05 \text{ (syst)}) \%$.

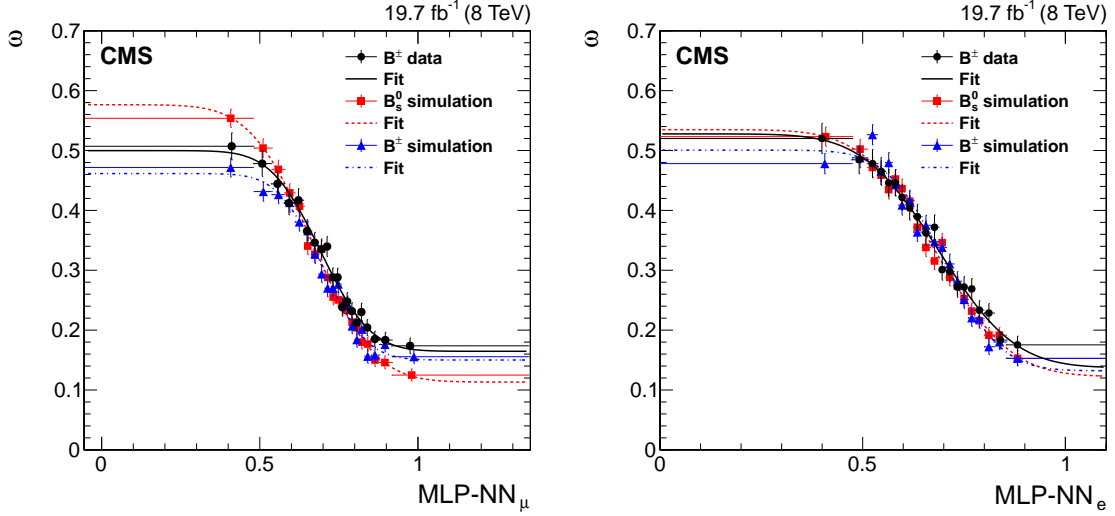


Figure 4: The mistag probabilities ω , defined as the ratio of the number of wrongly tagged events divided by the total number of tagged events, as a function of the MLP-NN discriminators for muons (left) and electrons (right). The data points (solid markers) are placed at the average weighted value of the events in each bin. The vertical bars show the statistical uncertainties and the horizontal bars the bin width. The solid line represents the parametrisation curve extracted from the background-subtracted B^\pm data; the dashed and dot-dashed lines refer to the parametrisations extracted from the simulated B_s^0 and B^\pm samples, respectively.

5 Maximum-likelihood fit

An unbinned maximum-likelihood fit to the data is performed by including the information on the B_s^0 invariant mass ($m_{B_s^0}$), the three decay angles (Θ) of the reconstructed B_s^0 candidates, the flavour tag decision (ζ), ct , and σ_{ct} , obtained by summing in quadrature the decay length uncertainty and the uncertainty in the transverse momentum. The fit is applied to the sample of 70 500 events, out of which 5 650 are tagged events, selected in the mass range 5.24–5.49 GeV and $ct = 200$ – $3\,000\ \mu\text{m}$. From this multidimensional fit, the physics parameters of interest $\Delta\Gamma_s$, ϕ_s , the B_s^0 mean lifetime $c\tau$, $|A_\perp|^2$, $|A_0|^2$, $|A_S|^2$, and the strong phases δ_\parallel , δ_\perp , and $\delta_{S\perp}$ are determined, where $\delta_{S\perp}$ is defined as the difference $\delta_S - \delta_\perp$. The P-wave amplitudes are normalised to unity by constraining $|A_\parallel|^2$ to $1 - |A_\perp|^2 - |A_0|^2$. The fit model is validated with simulated pseudo-experiments and with simulated samples with different parameter sets.

The likelihood function is composed of probability density functions (pdf) describing the signal and background components. The likelihood fit algorithm is implemented using the RooFit package from the ROOT framework [30]. The signal and background pdfs are formed as the product of pdfs that model the invariant mass distribution and the time-dependent decay rates of the reconstructed candidates. In addition, the signal pdf also includes the efficiency function. The event likelihood function \mathcal{L} is represented as:

$$\begin{aligned}\mathcal{L} &= L_s + L_{\text{bkg}}, \\ L_s &= N_s [\tilde{f}(\Theta, ct, \alpha) \otimes G(ct, \sigma_{ct}) \epsilon(\Theta)] P_s(m_{B_s^0}) P_s(\sigma_{ct}) P_s(\zeta), \\ L_{\text{bkg}} &= N_{\text{bkg}} P_{\text{bkg}}(\cos\theta_T, \varphi_T) P_{\text{bkg}}(\cos\psi_T) P_{\text{bkg}}(ct) P_{\text{bkg}}(m_{B_s^0}) P_{\text{bkg}}(\sigma_{ct}) P_{\text{bkg}}(\zeta),\end{aligned}$$

where L_s and L_{bkg} are the pdfs that describe the $B_s^0 \rightarrow J/\psi\phi(1020)$ signal and background contributions, respectively. The number of signal (background) events is N_s (N_{bkg}). The pdf $\tilde{f}(\Theta, ct, \alpha)$ is the differential decay rate function $f(\Theta, ct, \alpha)$ defined in Eq. (1), modified to in-

clude the flavour tagging information and the dilution term $(1 - 2\omega)$, which are applied to each of the c_i and d_i terms of the equation. In the \tilde{f} expression, the value of δ_0 is set to zero, following a general convention. The function $\epsilon(\Theta)$ is the angular efficiency and $G(ct, \sigma_{ct})$ is a Gaussian resolution function, which makes use of the event-by-event decay time uncertainty σ_{ct} , scaled by a factor κ . The κ factor is a function of ct and is introduced as a correction to take care of residual effects when the decay time uncertainty is used to model the ct resolution. The function $\kappa(ct)$ is measured using simulated samples and, on average, its value equals 1.0 to within a few percent. The average decay time uncertainty including the $\kappa(ct)$ factor equals 23.4 μm . All the parameters of the pdfs are left free to float in the final fit, unless explicitly stated otherwise. The value of $\Delta\Gamma_s$ is constrained to be positive, based on recent measurements [31].

The signal mass pdf $P_s(m_{B_s^0})$ is the sum of three Gaussian functions with a common mean; the two smaller widths, the mean, and the fraction of each Gaussian function are fixed to the values obtained in a one-dimensional mass fit. The background mass distribution $P_{\text{bkg}}(m_{B_s^0})$ is described by an exponential function. The background decay time component $P_{\text{bkg}}(ct)$ is described by the sum of two exponential functions. The angular parts of the backgrounds pdfs $P_{\text{bkg}}(\cos\theta_T, \varphi_T)$ and $P_{\text{bkg}}(\cos\psi_T)$ are described analytically by a series of Legendre polynomials for $\cos\theta_T$ and $\cos\psi_T$ and sinusoidal functions for φ_T . For the $\cos\theta_T$ and φ_T variables a two-dimensional pdf is used to take into account the correlation among the variables.

The signal decay time uncertainty pdf $P_s(\sigma_{ct})$ is a sum of two Gamma functions, with all the parameters fixed to the values obtained by fitting a sample of background-subtracted events. The background decay time uncertainty pdf $P_{\text{bkg}}(\sigma_{ct})$ is represented by a Gamma function. All the parameters are fixed to the values obtained by fitting the B_s^0 invariant mass sideband regions, defined by the mass ranges $m_{B_s^0} = 5.24\text{--}5.28\text{ GeV}$ and $5.45\text{--}5.49\text{ GeV}$. The functions $P_s(\xi)$ and $P_{\text{bkg}}(\xi)$ are the tag decision ξ pdfs, which have been obtained from the data.

6 Results and systematic uncertainties

The results of the fit are given in Table 2, where the quoted uncertainties are statistical only. The corresponding correlation matrix for the statistical uncertainties in the physics fit parameters is shown in Table 3. Since the likelihood profiles of δ_{\parallel} , $\delta_{S\perp}$, and $|A_S|^2$ are not parabolic, the statistical uncertainties quoted for these parameters are found from the increase in $-\log\mathcal{L}$ by 0.5. In the fit, the value of Δm_s is allowed to vary following a Gaussian distribution with mean and standard deviation set to $(17.69 \pm 0.08) \times 10^{12}\text{ h/s}$ [32]. As a cross-check, the Δm_s value is also left free to float and its best fit value is found to be in statistical agreement with the set value. The various data distributions and the fit projections are shown in Figs. 2, 3, and 5. The drop in the $\cos\theta_T$ distribution at the range limits is identified as being caused by close-by, high-angle kaon tracks. The central value and the 68%, 90%, and 95% confidence level (CL) likelihood contours of the fit in the $\Delta\Gamma_s\text{--}\phi_s$ plane are shown in Fig. 6.

Several sources of systematic uncertainties in the primary measured quantities are investigated by testing the various assumptions made in the fit model and those associated with the fit procedure.

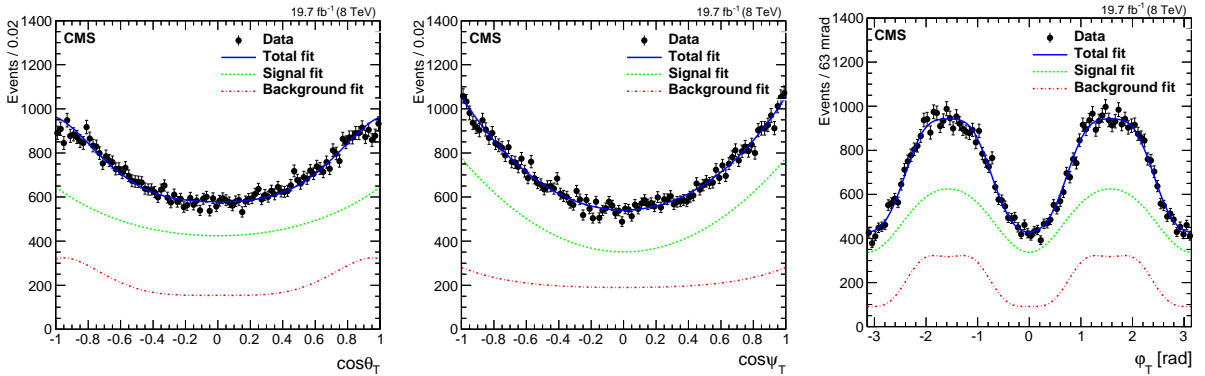
The systematic uncertainty associated with the assumption of a constant efficiency as a function of ct is evaluated by fitting the data with an alternative ct efficiency parametrisation, which takes into account a small contribution of the decay time significance requirement at small ct and first-order polynomial variations at high ct . The differences found in the fit results with respect to the nominal fit are used as systematic uncertainties.

Table 2: Results of the fit to the data. Uncertainties are statistical only.

Parameter	Fit result
ϕ_s [rad]	-0.075 ± 0.097
$\Delta\Gamma_s$ [ps^{-1}]	0.095 ± 0.013
$ A_0 ^2$	0.510 ± 0.005
$ A_S ^2$	$0.012^{+0.009}_{-0.007}$
$ A_{\perp} ^2$	0.243 ± 0.008
δ_{\parallel} [rad]	$3.48^{+0.07}_{-0.09}$
$\delta_{S\perp}$ [rad]	$0.37^{+0.28}_{-0.12}$
δ_{\perp} [rad]	2.98 ± 0.36
$c\tau$ [μm]	447.2 ± 2.9

Table 3: Correlation matrix for the statistical uncertainties in the physics fit parameters.

	$ A_0 ^2$	$ A_S ^2$	$ A_{\perp} ^2$	δ_{\parallel}	$\delta_{S\perp}$	δ_{\perp}	$c\tau$	$\Delta\Gamma_s$	ϕ_s
$ A_0 ^2$	+1.00	+0.19	-0.64	-0.08	-0.18	-0.02	+0.38	+0.70	+0.11
$ A_S ^2$	—	+1.00	-0.02	-0.32	-0.79	-0.10	-0.16	+0.01	+0.03
$ A_{\perp} ^2$	—	—	+1.00	-0.27	+0.03	-0.06	-0.50	-0.77	-0.11
δ_{\parallel}	—	—	—	+1.00	+0.26	+0.21	+0.11	+0.03	-0.02
$\delta_{S\perp}$	—	—	—	—	+1.00	+0.06	+0.11	-0.04	-0.06
δ_{\perp}	—	—	—	—	—	+1.00	+0.03	+0.01	+0.01
$c\tau$	—	—	—	—	—	—	+1.00	+0.55	+0.10
$\Delta\Gamma_s$	—	—	—	—	—	—	—	+1.00	+0.10
ϕ_s	—	—	—	—	—	—	—	—	+1.00

Figure 5: The angular distributions ($\cos\theta_T$, $\cos\psi_T$, ϕ_T) of the B_s^0 candidates from data (solid markers). The solid line is the result of the fit, the dashed line is the signal component, and the dot-dashed line is the background component.

The uncertainties associated with the variables $\cos\theta_T$, ϕ_T , and $\cos\psi_T$ of the 3D angular efficiency function are propagated to the fit results by varying the corresponding parameters within their statistical uncertainties, accounting for the correlations among the parameters. The maximum variation of the parameters extracted from the fit is taken as the systematic uncertainty. The systematic uncertainty owing to a small discrepancy in the kaon p_T spectrum between data and simulation is evaluated by weighting the events to make the simulated kaon p_T spectrum match that in data.

The uncertainty in the ct resolution associated with the κ factor is propagated to the results. A set of test samples is produced with the $\kappa(ct)$ factor varying within their uncertainty, assumed to be Gaussian. One standard deviation of the distribution describing the difference between

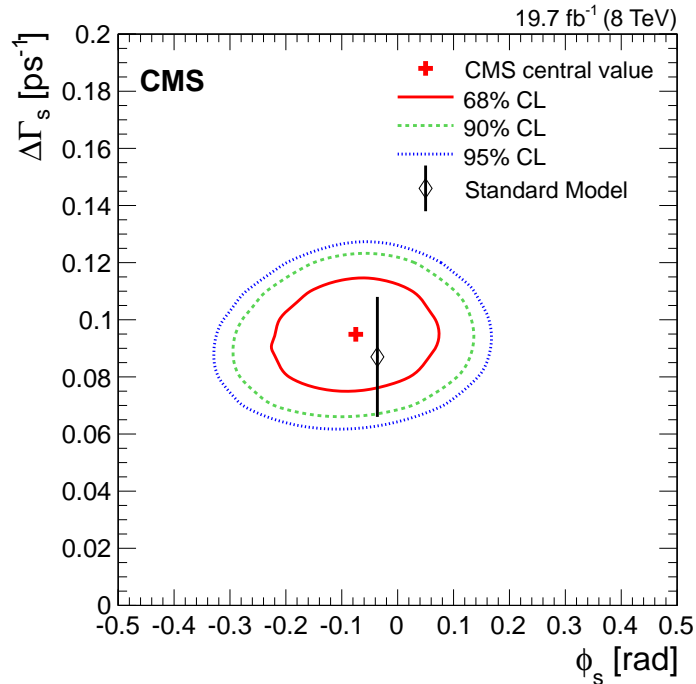


Figure 6: The CMS measured central value and the 68%, 90%, and 95% CL contours in the $\Delta\Gamma_s$ versus ϕ_s plane, together with the SM prediction [3, 4]. Uncertainties are statistical only.

the ct resolution with the nominal fit and with a varying $\kappa(ct)$ is taken as the systematic uncertainty. Since the $\kappa(ct)$ factor is obtained from simulation, the associated systematic uncertainty is assessed by using a sample of prompt J/ψ decays obtained with an unbiased trigger and comparing them to similarly processed simulated data. In this way the decay time resolution for $ct \approx 0$ is obtained. The $\kappa(ct)$ factor is varied within the values observed in data and simulation. The resulting variations of the physics parameters are taken as systematic uncertainties.

Although the likelihood function makes use of a per-event mistag parameter, it does not contain a pdf model for the mistag distribution. The associated systematic uncertainty is estimated by generating simulated pseudo-experiments with different mistag distributions for signal and background and fitting them with the nominal fit.

The dominant tagging systematic uncertainty originates from the assumption that the signal and calibration channels have the same tagging performance. It is evaluated using a calibration curve, obtained from simulated samples, that describes the mistag probability of B_s^0 as function of the mistag probability of B^\pm . The fit to the data is repeated, re-calibrating the mistag probability with the B_s^0 - B^\pm calibration curve, and the differences found in the fit results with respect to the nominal fit are used as the systematic uncertainties.

Possible biases intrinsic to the fit model are also taken into account. The nominal model function is tested by using simulated pseudo-experiments, and the average of the pulls (defined as the difference between the result of fit to the pseudo-experiment sample and the nominal value) is used as a systematic uncertainty if it exceeds one standard deviation statistical uncertainty.

The various hypotheses that have been assumed when building the likelihood function are tested by generating simulated pseudo-experiments with different hypotheses and fitting the samples with the nominal likelihood function. The obtained pull histograms of the physics variables are fitted with Gaussian functions, and the average of the pull is used as a systematic uncertainty if the difference with respect to the average exceeds one standard deviation

statistical uncertainty. Concerning the modelling of the $J/\psi K^+ K^-$ invariant mass distribution, the background model is changed to a Chebyshev function from the nominal exponential pdf. The ct background pdf is changed to the sum of three exponential functions instead of the two exponential functions of the nominal fit. The angular background pdf is generated by using the background simulation angular shapes instead of the fit ones. The effect of not including the angular resolution is also tested, using the residual distributions obtained from simulations. The RMS of the angular resolutions were found to be 5.9, 6.3, and 10 mrad, for $\cos\theta_T$, $\cos\psi_T$, and ϕ_T respectively. The contribution to the systematic uncertainty from the background tagging asymmetry is negligible.

The hypothesis that $|\lambda| = 1$ is tested by leaving that parameter free in the fit. The obtained value of $|\lambda|$ is consistent with 1.0 within one standard deviation. The differences found in the fit results with respect to the nominal fit are used as systematic uncertainties.

The alignment systematic uncertainty affects the vertex reconstruction and therefore the decay times. That effect is estimated to be $1.5 \mu\text{m}$ from studies of known B hadron lifetimes [33]. The systematic effect owing to the very small number of B_s^0 originating from $B_c^+ \rightarrow B_s^0 \pi^+$ feed-down, which would be reconstructed with large values of ct , has been found to be negligible.

The measured values for the weak phase ϕ_s and the decay width difference $\Delta\Gamma_s$ are:

$$\begin{aligned}\phi_s &= -0.075 \pm 0.097 \text{ (stat)} \pm 0.031 \text{ (syst) rad,} \\ \Delta\Gamma_s &= 0.095 \pm 0.013 \text{ (stat)} \pm 0.007 \text{ (syst) ps}^{-1}.\end{aligned}$$

The systematic uncertainties are summarised in Table 4. The uncertainties in the ϕ_s and $\Delta\Gamma_s$ results are dominated by the statistical uncertainties.

Table 4: Summary of the uncertainties in the measurements of the various B_s^0 parameters. If no value is reported, then the systematic uncertainty is negligible with respect to the statistical and other systematic uncertainties. The total systematic uncertainty is the quadratic sum of the listed systematic uncertainties.

Source of uncertainty	ϕ_s [rad]	$\Delta\Gamma_s$ [ps ⁻¹]	$ A_0 ^2$	$ A_S ^2$	$ A_\perp ^2$	δ_\parallel [rad]	$\delta_{S\perp}$ [rad]	δ_\perp [rad]	$c\tau$ [μm]
ct efficiency	0.002	0.0057	0.0015	—	0.0023	—	—	—	1.0
Angular efficiency	0.016	0.0021	0.0060	0.008	0.0104	0.674	0.14	0.66	0.8
Kaon p_T weighting	0.014	0.0015	0.0094	0.020	0.0041	0.085	0.11	0.02	1.1
ct resolution	0.006	0.0021	0.0009	—	0.0008	0.004	—	0.02	2.9
Mistag distribution modelling	0.004	0.0003	0.0006	—	—	0.008	0.01	—	0.1
Flavour tagging	0.003	0.0003	—	—	—	0.006	0.02	—	—
Model bias	0.015	0.0012	0.0008	—	—	0.025	0.03	—	0.4
pdf modelling assumptions	0.006	0.0021	0.0016	0.002	0.0021	0.010	0.03	0.04	0.2
$ \lambda $ as a free parameter	0.015	0.0003	0.0001	0.005	0.0001	0.002	0.01	0.03	—
Tracker alignment	—	—	—	—	—	—	—	—	1.5
Total systematic uncertainty	0.031	0.0070	0.0114	0.022	0.0116	0.680	0.18	0.66	3.7
Statistical uncertainty	0.097	0.0134	0.0053	0.008	0.0075	0.081	0.17	0.36	2.9

7 Summary

Using pp collision data collected by the CMS experiment at a centre-of-mass energy of 8 TeV and corresponding to an integrated luminosity of 19.7 fb^{-1} , 49 200 $B_s^0 \rightarrow J/\psi \phi(1020)$ signal candidates were used to measure the weak phase ϕ_s and the decay width difference $\Delta\Gamma_s$. The analysis was performed by using opposite-side lepton tagging of the B_s^0 flavour at the production time. Both muon and electron tags were used.

The measured values for the weak phase and the decay width difference between the B_s^0 mass eigenstates are $\phi_s = -0.075 \pm 0.097$ (stat) ± 0.031 (syst) rad and $\Delta\Gamma_s = 0.095 \pm 0.013$ (stat) ± 0.007 (syst) ps^{-1} , respectively. The measured values are consistent with those obtained by the LHCb Collaboration using $B_s^0 \rightarrow J/\psi K^+ K^-$ decays [34].

Our measured value of ϕ_s agrees with the SM prediction. Our result confirms $\Delta\Gamma_s$ to be nonzero, with a value consistent with theoretical predictions. The uncertainties in our ϕ_s and $\Delta\Gamma_s$ measurements are dominated by statistical uncertainties. Our results provide independent reference measurements of ϕ_s and $\Delta\Gamma_s$, and contribute to improving the overall precision of these quantities and thereby probing the SM further. Since our measurement precision is still limited by statistical uncertainty, substantial improvement is expected from LHC $\sqrt{s} = 13$ TeV high-luminosity running that will be available over the next few years.

Acknowledgments

We congratulate our colleagues in the CERN accelerator departments for the excellent performance of the LHC and thank the technical and administrative staffs at CERN and at other CMS institutes for their contributions to the success of the CMS effort. In addition, we gratefully acknowledge the computing centres and personnel of the Worldwide LHC Computing Grid for delivering so effectively the computing infrastructure essential to our analyses. Finally, we acknowledge the enduring support for the construction and operation of the LHC and the CMS detector provided by the following funding agencies: BMWFW and FWF (Austria); FNRS and FWO (Belgium); CNPq, CAPES, FAPERJ, and FAPESP (Brazil); MES (Bulgaria); CERN; CAS, MOST, and NSFC (China); COLCIENCIAS (Colombia); MSES and CSF (Croatia); RPF (Cyprus); MoER, ERC IUT and ERDF (Estonia); Academy of Finland, MEC, and HIP (Finland); CEA and CNRS/IN2P3 (France); BMBF, DFG, and HGF (Germany); GSRT (Greece); OTKA and NIH (Hungary); DAE and DST (India); IPM (Iran); SFI (Ireland); INFN (Italy); MSIP and NRF (Republic of Korea); LAS (Lithuania); MOE and UM (Malaysia); CINVESTAV, CONACYT, SEP, and UASLP-FAI (Mexico); MBIE (New Zealand); PAEC (Pakistan); MSHE and NSC (Poland); FCT (Portugal); JINR (Dubna); MON, RosAtom, RAS and RFBR (Russia); MESTD (Serbia); SEIDI and CPAN (Spain); Swiss Funding Agencies (Switzerland); MST (Taipei); ThEPCenter, IPST, STAR and NSTDA (Thailand); TUBITAK and TAEK (Turkey); NASU and SFFR (Ukraine); STFC (United Kingdom); DOE and NSF (USA).

Individuals have received support from the Marie-Curie programme and the European Research Council and EPLANET (European Union); the Leventis Foundation; the Alfred P. Sloan Foundation; the Alexander von Humboldt Foundation; the Belgian Federal Science Policy Office; the Fonds pour la Formation à la Recherche dans l'Industrie et dans l'Agriculture (FRIA-Belgium); the Agentschap voor Innovatie door Wetenschap en Technologie (IWT-Belgium); the Ministry of Education, Youth and Sports (MEYS) of the Czech Republic; the Council of Science and Industrial Research, India; the HOMING PLUS programme of the Foundation for Polish Science, cofinanced from European Union, Regional Development Fund; the Compagnia di San Paolo (Torino); the Consorzio per la Fisica (Trieste); MIUR project 20108T4XTM (Italy); the Thalís and Aristeia programmes cofinanced by EU-ESF and the Greek NSRF; the National Priorities Research Program by Qatar National Research Fund; the Rachadapisek Sompot Fund for Postdoctoral Fellowship, Chulalongkorn University (Thailand); and the Welch Foundation.

References

- [1] B. Bhattacharya, A. Datta, and D. London, “Reducing penguin pollution”, *Int. J. Mod. Phys. A* **28** (2013) 1350063, doi:10.1142/S0217751X13500632.
- [2] S. Faller, R. Fleischer, and T. Mannel, “Precision Physics with $B_s^0 \rightarrow J/\psi\phi$ at the LHC: The Quest for New Physics”, *Phys. Rev. D* **79** (2009) 014005, doi:10.1103/PhysRevD.79.014005, arXiv:0810.4248.
- [3] J. Charles et al., “Predictions of selected flavour observables within the standard model”, *Phys. Rev. D* **84** (2011) 033005, doi:10.1103/PhysRevD.84.033005, arXiv:1106.4041.
- [4] A. Lenz and U. Nierste, “Numerical updates of lifetimes and mixing parameters of B mesons”, in *Proceedings of the 6th International Workshop on the CKM Unitarity Triangle*, T. Gershon, ed. University of Warwick, United Kingdom, September, 2010. arXiv:1102.4274.
- [5] CDF Collaboration, “First Flavor-Tagged Determination of Bounds on Mixing-Induced CP Violation in $B_s^0 \rightarrow J/\psi\phi$ Decays”, *Phys. Rev. Lett.* **100** (2008) 161802, doi:10.1103/PhysRevLett.100.161802, arXiv:0712.2397.
- [6] D0 Collaboration, “Measurement of B_s^0 Mixing Parameters from the Flavor-Tagged Decay $B_s^0 \rightarrow J/\psi\phi$ ”, *Phys. Rev. Lett.* **101** (2008) 241801, doi:10.1103/PhysRevLett.101.241801, arXiv:0802.2255.
- [7] CDF Collaboration, “Measurement of the CP-violating phase $\beta_s^{J/\psi\phi}$ in $B_s^0 \rightarrow J/\psi\phi$ decays with the CDF II detector”, *Phys. Rev. D* **85** (2012) 072002, doi:10.1103/PhysRevD.85.072002, arXiv:1112.1726.
- [8] D0 Collaboration, “Measurement of the CP-violating phase $\phi_s^{J/\psi\phi}$ using the flavor-tagged decay $B_s^0 \rightarrow J/\psi\phi$ in 8 fb^{-1} of $p\bar{p}$ collisions”, *Phys. Rev. D* **85** (2012) 032006, doi:10.1103/PhysRevD.85.032006, arXiv:1109.3166.
- [9] LHCb Collaboration, “Measurement of the CP-violating phase ϕ_s in $\bar{B}_s^0 \rightarrow J/\psi\pi^+\pi^-$ decays”, *Phys. Lett. B* **736** (2014) 186, doi:10.1016/j.physletb.2014.06.079, arXiv:1405.4140.
- [10] LHCb Collaboration, “Measurement of CP violation and the B_s^0 meson decay width difference with $B_s^0 \rightarrow J/\psi K^+K^-$ and $B_s^0 \rightarrow J/\psi\pi^+\pi^-$ decays”, *Phys. Rev. D* **87** (2013) 112010, doi:10.1103/PhysRevD.87.112010, arXiv:1304.2600.
- [11] LHCb Collaboration, “Measurement of the CP-violating phase ϕ_s in $\bar{B}_s^0 \rightarrow J/\psi\pi^+\pi^-$ decays”, *Phys. Lett. B* **713** (2012) 378, doi:10.1016/j.physletb.2012.06.032, arXiv:1204.5675.
- [12] ATLAS Collaboration, “Time-dependent angular analysis of the decay $B_s^0 \rightarrow J/\psi\phi$ and extraction of $\Delta\Gamma_s$ and the CP-violating weak phase ϕ_s by ATLAS”, *JHEP* **12** (2012) 072, doi:10.1007/JHEP12(2012)072, arXiv:1208.0572.
- [13] ATLAS Collaboration, “Flavor tagged time-dependent angular analysis of the $B_s^0 \rightarrow J/\psi\phi$ decay and extraction of $\Delta\Gamma_s$ and the weak phase ϕ_s in ATLAS”, *Phys. Rev. D* **90** (2014) 052007, doi:10.1103/PhysRevD.90.052007.

- [14] A. S. Dighe, I. Dunietz, and R. Fleischer, “Extracting CKM phases and $B_s^0 - \bar{B}_s$ mixing parameters from angular distributions of non-leptonic B decays”, *Eur. Phys. J. C* **6** (1999) 647, doi:10.1007/s100529800954, arXiv:hep-ph/9804253.
- [15] A. S. Dighe, I. Dunietz, H. J. Lipkin, and J. L. Rosner, “Angular distributions and lifetime differences in $B_s^0 \rightarrow J/\psi\phi$ decays”, *Phys. Lett. B* **369** (1996) 144, doi:10.1016/0370-2693(95)01523-X, arXiv:hep-ph/9511363.
- [16] G. Branco, L. Lavoura, and J. Silva, “CP violation”. Clarendon Press, Oxford, 1999. Int. Ser. Monogr. Phys. (103).
- [17] LHCb Collaboration, “Measurement of the flavour-specific CP-violating asymmetry a_{sl}^s in B_s^0 decays”, *Phys. Lett. B* **728** (2014) 607, doi:10.1016/j.physletb.2013.12.030, arXiv:1308.1048.
- [18] CMS Collaboration, “Description and performance of track and primary-vertex reconstruction with the CMS tracker”, *JINST* **9** (2014) P10009, doi:10.1088/1748-0221/9/10/P10009, arXiv:1405.6569.
- [19] CMS Collaboration, “Performance of CMS muon reconstruction in pp collision events at $\sqrt{s} = 7$ TeV”, *JINST* **7** (2012) P10002, doi:10.1088/1748-0221/7/10/P10002, arXiv:1206.4071.
- [20] CMS Collaboration, “The CMS experiment at the CERN LHC”, *JINST* **3** (2008) S08004, doi:10.1088/1748-0221/3/08/S08004.
- [21] Particle Data Group, K. A. Olive et al., “Review of Particle Physics”, *Chin. Phys. C* **38** (2014) 090001, doi:10.1088/1674-1137/38/9/090001.
- [22] T. Sjöstrand, S. Mrenna, and P. Z. Skands, “PYTHIA 6.4 physics and manual”, *JHEP* **05** (2006) 026, doi:10.1088/1126-6708/2006/05/026, arXiv:hep-ph/0603175.
- [23] D. J. Lange, “The EvtGen particle decay simulation package”, *Nucl. Instrum. Meth. A* **462** (2001) 152, doi:10.1016/S0168-9002(01)00089-4.
- [24] E. Barberio, B. van Eijk, and Z. Was, “PHOTOS – a universal Monte Carlo for QED radiative corrections in decays”, *Comp. Phys. Commun.* **66** (1991) 115, doi:10.1016/0010-4655(91)90012-A.
- [25] E. Barberio and Z. Was, “PHOTOS – a universal Monte Carlo for QED radiative corrections: version 2.0”, *Comp. Phys. Commun.* **79** (1994) 291, doi:10.1016/0010-4655(94)90074-4.
- [26] GEANT4 Collaboration, “GEANT4—a simulation toolkit”, *Nucl. Instrum. Meth. A* **506** (2003) 250, doi:10.1016/S0168-9002(03)01368-8.
- [27] CMS Collaboration, “Particle-Flow Event Reconstruction in CMS and Performance for Jets, Taus, and E_T^{miss} ”, CMS Physics Analysis Summary CMS-PAS-PFT-09-001, 2009.
- [28] CMS Collaboration, “Commissioning of the Particle-flow Event Reconstruction with the first LHC collisions recorded in the CMS detector”, CMS Physics Analysis Summary CMS-PAS-PFT-10-001, 2010.
- [29] H. Voss, A. Höcker, J. Stelzer, and F. Tegenfeldt, “TMVA, the Toolkit for Multivariate Data Analysis with ROOT”, in *Xith International Workshop on Advanced Computing and Analysis Techniques in Physics Research (ACAT)*, p. 40. 2007. arXiv:physics/0703039.

- [30] I. Antcheva et al., “ROOT — A C++ framework for petabyte data storage, statistical analysis and visualization”, *Comp. Phys. Commun.* **180** (2009) 2499, doi:10.1016/j.cpc.2009.08.005.
- [31] LHCb Collaboration, “Determination of the Sign of the Decay Width Difference in the B_s^0 System”, *Phys. Rev. Lett.* **108** (2012) 241801, doi:10.1103/PhysRevLett.108.241801, arXiv:1202.4717.
- [32] Particle Data Group, J. Beringer et al., “Review of Particle Physics”, *Phys. Rev. D* **86** (2012) 010001, doi:10.1103/PhysRevD.86.010001.
- [33] CMS Collaboration, “Measurement of the Λ_b^0 lifetime in pp collisions at $\sqrt{s} = 7$ TeV”, *J. High Energy Phys.* **07** (2013) 163, doi:10.1007/JHEP07(2013)163.
- [34] LHCb Collaboration, “Precision Measurement of CP Violation in $B_s^0 \rightarrow J/\psi K^+ K^-$ Decays”, *Phys. Rev. Lett.* **114** (2015) 041801, doi:10.1103/PhysRevLett.114.041801, arXiv:1411.3104.

A The CMS Collaboration

Yerevan Physics Institute, Yerevan, Armenia

V. Khachatryan, A.M. Sirunyan, A. Tumasyan

Institut für Hochenergiephysik der OeAW, Wien, Austria

W. Adam, E. Asilar, T. Bergauer, J. Brandstetter, E. Brondolin, M. Dragicevic, J. Erö, M. Flechl, M. Friedl, R. Frühwirth¹, V.M. Ghete, C. Hartl, N. Hörmann, J. Hrubec, M. Jeitler¹, V. Knünz, A. König, M. Krammer¹, I. Krätschmer, D. Liko, T. Matsushita, I. Mikulec, D. Rabady², B. Rahbaran, H. Rohringer, J. Schieck¹, R. Schöfbeck, J. Strauss, W. Treberer-Treberspurg, W. Waltenberger, C.-E. Wulz¹

National Centre for Particle and High Energy Physics, Minsk, Belarus

V. Mossolov, N. Shumeiko, J. Suarez Gonzalez

Universiteit Antwerpen, Antwerpen, Belgium

S. Alderweireldt, T. Cornelis, E.A. De Wolf, X. Janssen, A. Knutsson, J. Lauwers, S. Luyckx, S. Ochesanu, R. Rougny, M. Van De Klundert, H. Van Haevermaet, P. Van Mechelen, N. Van Remortel, A. Van Spilbeek

Vrije Universiteit Brussel, Brussel, Belgium

S. Abu Zeid, F. Blekman, J. D'Hondt, N. Daci, I. De Bruyn, K. Deroover, N. Heracleous, J. Keaveney, S. Lowette, L. Moreels, A. Olbrechts, Q. Python, D. Strom, S. Tavernier, W. Van Doninck, P. Van Mulders, G.P. Van Onsem, I. Van Parijs

Université Libre de Bruxelles, Bruxelles, Belgium

P. Barria, H. Brun, C. Caillol, B. Clerbaux, G. De Lentdecker, H. Delannoy, G. Fasanella, L. Favart, A.P.R. Gay, A. Grebenyuk, G. Karapostoli, T. Lenzi, A. Léonard, T. Maerschalk, A. Marinov, L. Perniè, A. Randle-conde, T. Reis, T. Seva, C. Vander Velde, P. Vanlaer, R. Yonamine, F. Zenoni, F. Zhang³

Ghent University, Ghent, Belgium

K. Beernaert, L. Benucci, A. Cimmino, S. Crucy, D. Dobur, A. Fagot, G. Garcia, M. Gul, J. Mccartin, A.A. Ocampo Rios, D. Poyraz, D. Ryckbosch, S. Salva, M. Sigamani, N. Strobbe, M. Tytgat, W. Van Driessche, E. Yazgan, N. Zaganidis

Université Catholique de Louvain, Louvain-la-Neuve, Belgium

S. Basesmez, C. Beluffi⁴, O. Bondu, S. Brochet, G. Bruno, R. Castello, A. Caudron, L. Ceard, G.G. Da Silveira, C. Delaere, D. Favart, L. Forthomme, A. Giammanco⁵, J. Hollar, A. Jafari, P. Jez, M. Komm, V. Lemaitre, A. Mertens, C. Nuttens, L. Perrini, A. Pin, K. Piotrkowski, A. Popov⁶, L. Quertenmont, M. Selvaggi, M. Vidal Marono

Université de Mons, Mons, Belgium

N. Belyi, G.H. Hammad

Centro Brasileiro de Pesquisas Fisicas, Rio de Janeiro, Brazil

W.L. Aldá Júnior, G.A. Alves, L. Brito, M. Correa Martins Junior, M. Hamer, C. Hensel, C. Mora Herrera, A. Moraes, M.E. Pol, P. Rebello Teles

Universidade do Estado do Rio de Janeiro, Rio de Janeiro, Brazil

E. Belchior Batista Das Chagas, W. Carvalho, J. Chinellato⁷, A. Custódio, E.M. Da Costa, D. De Jesus Damiao, C. De Oliveira Martins, S. Fonseca De Souza, L.M. Huertas Guativa, H. Malbouisson, D. Matos Figueiredo, L. Mundim, H. Nogima, W.L. Prado Da Silva, A. Santoro, A. Sznajder, E.J. Tonelli Manganote⁷, A. Vilela Pereira

Universidade Estadual Paulista ^a, Universidade Federal do ABC ^b, São Paulo, Brazil

S. Ahuja^a, C.A. Bernardes^b, A. De Souza Santos^b, S. Dogra^a, T.R. Fernandez Perez Tomei^a, E.M. Gregores^b, P.G. Mercadante^b, C.S. Moon^{a,8}, S.F. Novaes^a, Sandra S. Padula^a, D. Romero Abad, J.C. Ruiz Vargas

Institute for Nuclear Research and Nuclear Energy, Sofia, Bulgaria

A. Aleksandrov, R. Hadjiiska, P. Iaydjiev, M. Rodozov, S. Stoykova, G. Sultanov, M. Vutova

University of Sofia, Sofia, Bulgaria

A. Dimitrov, I. Glushkov, L. Litov, B. Pavlov, P. Petkov

Institute of High Energy Physics, Beijing, China

M. Ahmad, J.G. Bian, G.M. Chen, H.S. Chen, M. Chen, T. Cheng, R. Du, C.H. Jiang, R. Plestina⁹, F. Romeo, S.M. Shaheen, J. Tao, C. Wang, Z. Wang, H. Zhang

State Key Laboratory of Nuclear Physics and Technology, Peking University, Beijing, China

C. Asawatrangkuldee, Y. Ban, Q. Li, S. Liu, Y. Mao, S.J. Qian, D. Wang, Z. Xu, W. Zou

Universidad de Los Andes, Bogota, Colombia

C. Avila, A. Cabrera, L.F. Chaparro Sierra, C. Florez, J.P. Gomez, B. Gomez Moreno, J.C. Sanabria

University of Split, Faculty of Electrical Engineering, Mechanical Engineering and Naval Architecture, Split, Croatia

N. Godinovic, D. Lelas, I. Puljak, P.M. Ribeiro Cipriano

University of Split, Faculty of Science, Split, Croatia

Z. Antunovic, M. Kovac

Institute Rudjer Boskovic, Zagreb, Croatia

V. Brigljevic, K. Kadija, J. Luetic, S. Micanovic, L. Sudic

University of Cyprus, Nicosia, Cyprus

A. Attikis, G. Mavromanolakis, J. Mousa, C. Nicolaou, F. Ptochos, P.A. Razis, H. Rykaczewski

Charles University, Prague, Czech Republic

M. Bodlak, M. Finger¹⁰, M. Finger Jr.¹⁰

Academy of Scientific Research and Technology of the Arab Republic of Egypt, Egyptian Network of High Energy Physics, Cairo, Egypt

M. El Sawy^{11,12}, E. El-khateeb^{13,13}, T. Elkafrawy¹³, A. Mohamed¹⁴, A. Radi^{12,13}, E. Salama^{12,13}

National Institute of Chemical Physics and Biophysics, Tallinn, Estonia

B. Calpas, M. Kadastik, M. Murumaa, M. Raidal, A. Tiko, C. Veelken

Department of Physics, University of Helsinki, Helsinki, Finland

P. Eerola, J. Pekkanen, M. Voutilainen

Helsinki Institute of Physics, Helsinki, Finland

J. Härkönen, T. Jarvinen, V. Karimäki, R. Kinnunen, T. Lampén, K. Lassila-Perini, S. Lehti, T. Lindén, P. Luukka, T. Mäenpää, T. Peltola, E. Tuominen, J. Tuominiemi, E. Tuovinen, L. Wendland

Lappeenranta University of Technology, Lappeenranta, Finland

J. Talvitie, T. Tuuva

DSM/IRFU, CEA/Saclay, Gif-sur-Yvette, France

M. Besancon, F. Couderc, M. Dejardin, D. Denegri, B. Fabbro, J.L. Faure, C. Favaro, F. Ferri, S. Ganjour, A. Givernaud, P. Gras, G. Hamel de Monchenault, P. Jarry, E. Locci, M. Machet, J. Malcles, J. Rander, A. Rosowsky, M. Titov, A. Zghiche

Laboratoire Leprince-Ringuet, Ecole Polytechnique, IN2P3-CNRS, Palaiseau, France

I. Antropov, S. Baffioni, F. Beaudette, P. Busson, L. Cadamuro, E. Chapon, C. Charlot, T. Dahms, O. Davignon, N. Filipovic, A. Florent, R. Granier de Cassagnac, S. Lisniak, L. Mastrolorenzo, P. Miné, I.N. Naranjo, M. Nguyen, C. Ochando, G. Ortona, P. Paganini, P. Pigard, S. Regnard, R. Salerno, J.B. Sauvan, Y. Sirois, T. Strebler, Y. Yilmaz, A. Zabi

Institut Pluridisciplinaire Hubert Curien, Université de Strasbourg, Université de Haute Alsace Mulhouse, CNRS/IN2P3, Strasbourg, France

J.-L. Agram¹⁵, J. Andrea, A. Aubin, D. Bloch, J.-M. Brom, M. Buttignol, E.C. Chabert, N. Chanon, C. Collard, E. Conte¹⁵, X. Coubez, J.-C. Fontaine¹⁵, D. Gelé, U. Goerlach, C. Goetzmann, A.-C. Le Bihan, J.A. Merlin², K. Skovpen, P. Van Hove

Centre de Calcul de l'Institut National de Physique Nucleaire et de Physique des Particules, CNRS/IN2P3, Villeurbanne, France

S. Gadrat

Université de Lyon, Université Claude Bernard Lyon 1, CNRS-IN2P3, Institut de Physique Nucléaire de Lyon, Villeurbanne, France

S. Beauceron, C. Bernet, G. Boudoul, E. Bouvier, C.A. Carrillo Montoya, R. Chierici, D. Contardo, B. Courbon, P. Depasse, H. El Mamouni, J. Fan, J. Fay, S. Gascon, M. Gouzevitch, B. Ille, F. Lagarde, I.B. Laktineh, M. Lethuillier, L. Mirabito, A.L. Pequegnot, S. Perries, J.D. Ruiz Alvarez, D. Sabes, L. Sgandurra, V. Sordini, M. Vander Donckt, P. Verdier, S. Viret, H. Xiao

Georgian Technical University, Tbilisi, Georgia

T. Toriashvili¹⁶

Tbilisi State University, Tbilisi, Georgia

Z. Tsamalaidze¹⁰

RWTH Aachen University, I. Physikalisches Institut, Aachen, Germany

C. Autermann, S. Beranek, M. Edelhoff, L. Feld, A. Heister, M.K. Kiesel, K. Klein, M. Lipinski, A. Ostapchuk, M. Preuten, F. Raupach, S. Schael, J.F. Schulte, T. Verlage, H. Weber, B. Wittmer, V. Zhukov⁶

RWTH Aachen University, III. Physikalisches Institut A, Aachen, Germany

M. Ata, M. Brodski, E. Dietz-Laursonn, D. Duchardt, M. Endres, M. Erdmann, S. Erdweg, T. Esch, R. Fischer, A. Güth, T. Hebbeker, C. Heidemann, K. Hoepfner, D. Klingebiel, S. Knutzen, P. Kreuzer, M. Merschmeyer, A. Meyer, P. Millet, M. Olschewski, K. Padeken, P. Papacz, T. Pook, M. Radziej, H. Reithler, M. Rieger, F. Scheuch, L. Sonnenschein, D. Teyssier, S. Thüer

RWTH Aachen University, III. Physikalisches Institut B, Aachen, Germany

V. Cherepanov, Y. Erdogan, G. Flügge, H. Geenen, M. Geisler, F. Hoehle, B. Kargoll, T. Kress, Y. Kuessel, A. Künsken, J. Lingemann², A. Nehr Korn, A. Nowack, I.M. Nugent, C. Pistone, O. Pooth, A. Stahl

Deutsches Elektronen-Synchrotron, Hamburg, Germany

M. Aldaya Martin, I. Asin, N. Bartosik, O. Behnke, U. Behrens, A.J. Bell, K. Borras, A. Burgmeier, A. Cakir, L. Calligaris, A. Campbell, S. Choudhury, F. Costanza, C. Diez

Pardos, G. Dolinska, S. Dooling, T. Dorland, G. Eckerlin, D. Eckstein, T. Eichhorn, G. Flucke, E. Gallo¹⁷, J. Garay Garcia, A. Geiser, A. Gizhko, P. Gunnellini, J. Hauk, M. Hempel¹⁸, H. Jung, A. Kalogeropoulos, O. Karacheban¹⁸, M. Kasemann, P. Katsas, J. Kieseler, C. Kleinwort, I. Korol, W. Lange, J. Leonard, K. Lipka, A. Lobanov, W. Lohmann¹⁸, R. Mankel, I. Marfin¹⁸, I.-A. Melzer-Pellmann, A.B. Meyer, G. Mittag, J. Mnich, A. Mussgiller, S. Naumann-Emme, A. Nayak, E. Ntomari, H. Perrey, D. Pitzl, R. Placakyte, A. Raspereza, B. Roland, M.Ö. Sahin, P. Saxena, T. Schoerner-Sadenius, M. Schröder, C. Seitz, S. Spannagel, K.D. Trippkewitz, R. Walsh, C. Wissing

University of Hamburg, Hamburg, Germany

V. Blobel, M. Centis Vignali, A.R. Draeger, J. Erfle, E. Garutti, K. Goebel, D. Gonzalez, M. Görner, J. Haller, M. Hoffmann, R.S. Höing, A. Junkes, R. Klanner, R. Kogler, T. Lapsien, T. Lenz, I. Marchesini, D. Marconi, M. Meyer, D. Nowatschin, J. Ott, F. Pantaleo², T. Peiffer, A. Perieanu, N. Pietsch, J. Poehlsen, D. Rathjens, C. Sander, H. Schettler, P. Schleper, E. Schlieckau, A. Schmidt, J. Schwandt, M. Seidel, V. Sola, H. Stadie, G. Steinbrück, H. Tholen, D. Troendle, E. Usai, L. Vanelderen, A. Vanhoefer, B. Vormwald

Institut für Experimentelle Kernphysik, Karlsruhe, Germany

M. Akbiyik, C. Barth, C. Baus, J. Berger, C. Böser, E. Butz, T. Chwalek, F. Colombo, W. De Boer, A. Descroix, A. Dierlamm, S. Fink, F. Frensch, M. Giffels, A. Gilbert, F. Hartmann², S.M. Heindl, U. Husemann, I. Katkov⁶, A. Kornmayer², P. Lobelle Pardo, B. Maier, H. Mildner, M.U. Mozer, T. Müller, Th. Müller, M. Plagge, G. Quast, K. Rabbertz, S. Röcker, F. Roscher, H.J. Simonis, F.M. Stober, R. Ulrich, J. Wagner-Kuhr, S. Wayand, M. Weber, T. Weiler, C. Wöhrmann, R. Wolf

Institute of Nuclear and Particle Physics (INPP), NCSR Demokritos, Aghia Paraskevi, Greece

G. Anagnostou, G. Daskalakis, T. Gerasis, V.A. Giakoumopoulou, A. Kyriakis, D. Loukas, A. Psallidas, I. Topsis-Giotis

University of Athens, Athens, Greece

A. Agapitos, S. Kesisoglou, A. Panagiotou, N. Saoulidou, E. Tziaferi

University of Ioánnina, Ioánnina, Greece

I. Evangelou, G. Flouris, C. Foudas, P. Kokkas, N. Loukas, N. Manthos, I. Papadopoulos, E. Paradas, J. Strologas

Wigner Research Centre for Physics, Budapest, Hungary

G. Bencze, C. Hajdu, A. Hazi, P. Hidas, D. Horvath¹⁹, F. Sikler, V. Veszpremi, G. Vesztergombi²⁰, A.J. Zsigmond

Institute of Nuclear Research ATOMKI, Debrecen, Hungary

N. Beni, S. Czellar, J. Karancsi²¹, J. Molnar, Z. Szillasi

University of Debrecen, Debrecen, Hungary

M. Bartók²², A. Makovec, P. Raics, Z.L. Trocsanyi, B. Ujvari

National Institute of Science Education and Research, Bhubaneswar, India

P. Mal, K. Mandal, N. Sahoo, S.K. Swain

Panjab University, Chandigarh, India

S. Bansal, S.B. Beri, V. Bhatnagar, R. Chawla, R. Gupta, U. Bhawandeep, A.K. Kalsi, A. Kaur, M. Kaur, R. Kumar, A. Mehta, M. Mittal, J.B. Singh, G. Walia

University of Delhi, Delhi, India

Ashok Kumar, A. Bhardwaj, B.C. Choudhary, R.B. Garg, A. Kumar, S. Malhotra, M. Naimuddin, N. Nishu, K. Ranjan, R. Sharma, V. Sharma

Saha Institute of Nuclear Physics, Kolkata, India

S. Banerjee, R. Bhardwaj, S. Bhattacharya, K. Chatterjee, S. Dey, S. Dutta, Sa. Jain, N. Majumdar, A. Modak, K. Mondal, S. Mukherjee, S. Mukhopadhyay, A. Roy, D. Roy, S. Roy Chowdhury, S. Sarkar, M. Sharan

Bhabha Atomic Research Centre, Mumbai, India

A. Abdulsalam, R. Chudasama, D. Dutta, V. Jha, V. Kumar, A.K. Mohanty², L.M. Pant, P. Shukla, A. Topkar

Tata Institute of Fundamental Research, Mumbai, India

T. Aziz, S. Banerjee, S. Bhowmik²³, R.M. Chatterjee, R.K. Dewanjee, S. Dugad, S. Ganguly, S. Ghosh, M. Guchait, A. Gurtu²⁴, G. Kole, S. Kumar, B. Mahakud, M. Maity²³, G. Majumder, K. Mazumdar, S. Mitra, G.B. Mohanty, B. Parida, T. Sarkar²³, K. Sudhakar, N. Sur, B. Sutar, N. Wickramage²⁵

Indian Institute of Science Education and Research (IISER), Pune, India

S. Chauhan, S. Dube, S. Sharma

Institute for Research in Fundamental Sciences (IPM), Tehran, Iran

H. Bakhshiansohi, H. Behnamian, S.M. Etesami²⁶, A. Fahim²⁷, R. Goldouzian, M. Khakzad, M. Mohammadi Najafabadi, M. Naseri, S. Paktinat Mehdiabadi, F. Rezaei Hosseinabadi, B. Safarzadeh²⁸, M. Zeinali

University College Dublin, Dublin, Ireland

M. Felcini, M. Grunewald

INFN Sezione di Bari ^a, Università di Bari ^b, Politecnico di Bari ^c, Bari, Italy

M. Abbrescia^{a,b}, C. Calabria^{a,b}, C. Caputo^{a,b}, A. Colaleo^a, D. Creanza^{a,c}, L. Cristella^{a,b}, N. De Filippis^{a,c}, M. De Palma^{a,b}, L. Fiore^a, G. Iaselli^{a,c}, G. Maggi^{a,c}, M. Maggi^a, G. Miniello^{a,b}, S. My^{a,c}, S. Nuzzo^{a,b}, A. Pompili^{a,b}, G. Pugliese^{a,c}, R. Radogna^{a,b}, A. Ranieri^a, G. Selvaggi^{a,b}, L. Silvestris^{a,2}, R. Venditti^{a,b}, P. Verwilligen^a

INFN Sezione di Bologna ^a, Università di Bologna ^b, Bologna, Italy

G. Abbiendi^a, C. Battilana², A.C. Benvenuti^a, D. Bonacorsi^{a,b}, S. Braibant-Giacomelli^{a,b}, L. Brigliadori^{a,b}, R. Campanini^{a,b}, P. Capiluppi^{a,b}, A. Castro^{a,b}, F.R. Cavallo^a, S.S. Chhibra^{a,b}, G. Codispoti^{a,b}, M. Cuffiani^{a,b}, G.M. Dallavalle^a, F. Fabbri^a, A. Fanfani^{a,b}, D. Fasanella^{a,b}, P. Giacomelli^a, C. Grandi^a, L. Guiducci^{a,b}, S. Marcellini^a, G. Masetti^a, A. Montanari^a, F.L. Navarria^{a,b}, A. Perrotta^a, A.M. Rossi^{a,b}, T. Rovelli^{a,b}, G.P. Siroli^{a,b}, N. Tosi^{a,b}, R. Travaglini^{a,b}

INFN Sezione di Catania ^a, Università di Catania ^b, CSFNSM ^c, Catania, Italy

G. Cappello^a, M. Chiorboli^{a,b}, S. Costa^{a,b}, F. Giordano^{a,b}, R. Potenza^{a,b}, A. Tricomi^{a,b}, C. Tuve^{a,b}

INFN Sezione di Firenze ^a, Università di Firenze ^b, Firenze, Italy

G. Barbagli^a, V. Ciulli^{a,b}, C. Civinini^a, R. D'Alessandro^{a,b}, E. Focardi^{a,b}, S. Gonzi^{a,b}, V. Gori^{a,b}, P. Lenzi^{a,b}, M. Meschini^a, S. Paoletti^a, G. Sguazzoni^a, A. Tropiano^{a,b}, L. Viliani^{a,b}

INFN Laboratori Nazionali di Frascati, Frascati, Italy

L. Benussi, S. Bianco, F. Fabbri, D. Piccolo, F. Primavera

INFN Sezione di Genova ^a, Università di Genova ^b, Genova, Italy

V. Calvelli^{a,b}, F. Ferro^a, M. Lo Vetere^{a,b}, M.R. Monge^{a,b}, E. Robutti^a, S. Tosi^{a,b}

INFN Sezione di Milano-Bicocca ^a, Università di Milano-Bicocca ^b, Milano, Italy

L. Brianza, M.E. Dinardo^{a,b}, S. Fiorendi^{a,b}, S. Gennai^a, R. Gerosa^{a,b}, A. Ghezzi^{a,b}, P. Govoni^{a,b}, S. Malvezzi^a, R.A. Manzoni^{a,b}, B. Marzocchi^{a,b,2}, D. Menasce^a, L. Moroni^a, M. Paganoni^{a,b}, D. Pedrini^a, S. Ragazzi^{a,b}, N. Redaelli^a, T. Tabarelli de Fatis^{a,b}

INFN Sezione di Napoli ^a, Università di Napoli 'Federico II' ^b, Napoli, Italy, Università della Basilicata ^c, Potenza, Italy, Università G. Marconi ^d, Roma, Italy

S. Buontempo^a, N. Cavallo^{a,c}, S. Di Guida^{a,d,2}, M. Esposito^{a,b}, F. Fabozzi^{a,c}, A.O.M. Iorio^{a,b}, G. Lanza^a, L. Lista^a, S. Meola^{a,d,2}, M. Merola^a, P. Paolucci^{a,2}, C. Sciacca^{a,b}, F. Thyssen

INFN Sezione di Padova ^a, Università di Padova ^b, Padova, Italy, Università di Trento ^c, Trento, Italy

P. Azzi^{a,2}, N. Bacchetta^a, L. Benato^{a,b}, D. Bisello^{a,b}, A. Boletti^{a,b}, R. Carlin^{a,b}, P. Checchia^a, M. Dall'Osso^{a,b,2}, T. Dorigo^a, F. Gasparini^{a,b}, U. Gasparini^{a,b}, F. Gonella^a, A. Gozzelino^a, K. Kanishchev^{a,c}, S. Lacaprara^a, M. Margoni^{a,b}, G. Maron^{a,29}, A.T. Meneguzzo^{a,b}, M. Michelotto^a, J. Pazzini^{a,b}, N. Pozzobon^{a,b}, P. Ronchese^{a,b}, F. Simonetto^{a,b}, E. Torassa^a, M. Tosi^{a,b}, M. Zanetti, P. Zotto^{a,b}, A. Zucchetta^{a,b,2}, G. Zumerle^{a,b}

INFN Sezione di Pavia ^a, Università di Pavia ^b, Pavia, Italy

A. Braghieri^a, A. Magnani^a, P. Montagna^{a,b}, S.P. Ratti^{a,b}, V. Re^a, C. Riccardi^{a,b}, P. Salvini^a, I. Vai^a, P. Vitulo^{a,b}

INFN Sezione di Perugia ^a, Università di Perugia ^b, Perugia, Italy

L. Alunni Solestizi^{a,b}, M. Biasini^{a,b}, G.M. Bilei^a, D. Ciangottini^{a,b,2}, L. Fanò^{a,b}, P. Lariccia^{a,b}, G. Mantovani^{a,b}, M. Menichelli^a, A. Saha^a, A. Santocchia^{a,b}, A. Spiezia^{a,b}

INFN Sezione di Pisa ^a, Università di Pisa ^b, Scuola Normale Superiore di Pisa ^c, Pisa, Italy

K. Androsov^{a,30}, P. Azzurri^a, G. Bagliesi^a, J. Bernardini^a, T. Boccali^a, G. Broccolo^{a,c}, R. Castaldi^a, M.A. Ciocci^{a,30}, R. Dell'Orso^a, S. Donato^{a,c,2}, G. Fedi, L. Foà^{a,c†}, A. Giassi^a, M.T. Grippo^{a,30}, F. Ligabue^{a,c}, T. Lomtadze^a, L. Martini^{a,b}, A. Messineo^{a,b}, F. Palla^a, A. Rizzi^{a,b}, A. Savoy-Navarro^{a,31}, A.T. Serban^a, P. Spagnolo^a, P. Squillacioti^{a,30}, R. Tenchini^a, G. Tonelli^{a,b}, A. Venturi^a, P.G. Verdini^a

INFN Sezione di Roma ^a, Università di Roma ^b, Roma, Italy

L. Barone^{a,b}, F. Cavallari^a, G. D'imperio^{a,b,2}, D. Del Re^{a,b}, M. Diemoz^a, S. Gelli^{a,b}, C. Jorda^a, E. Longo^{a,b}, F. Margaroli^{a,b}, P. Meridiani^a, G. Organtini^{a,b}, R. Paramatti^a, F. Preiato^{a,b}, S. Rahatlou^{a,b}, C. Rovelli^a, F. Santanastasio^{a,b}, P. Traczyk^{a,b,2}

INFN Sezione di Torino ^a, Università di Torino ^b, Torino, Italy, Università del Piemonte Orientale ^c, Novara, Italy

N. Amapane^{a,b}, R. Arcidiacono^{a,c,2}, S. Argiro^{a,b}, M. Arneodo^{a,c}, R. Bellan^{a,b}, C. Biino^a, N. Cartiglia^a, M. Costa^{a,b}, R. Covarelli^{a,b}, A. Degano^{a,b}, G. Dellacasa^a, N. Demaria^a, L. Finco^{a,b,2}, C. Mariotti^a, S. Maselli^a, E. Migliore^{a,b}, V. Monaco^{a,b}, E. Monteil^{a,b}, M. Musich^a, M.M. Obertino^{a,b}, L. Pacher^{a,b}, N. Pastrone^a, M. Pelliccioni^a, G.L. Pinna Angioni^{a,b}, F. Ravera^{a,b}, A. Romero^{a,b}, M. Ruspa^{a,c}, R. Sacchi^{a,b}, A. Solano^{a,b}, A. Staiano^a, U. Tamponi^a

INFN Sezione di Trieste ^a, Università di Trieste ^b, Trieste, Italy

S. Belforte^a, V. Candelise^{a,b,2}, M. Casarsa^a, F. Cossutti^a, G. Della Ricca^{a,b}, B. Gobbo^a, C. La Licata^{a,b}, M. Marone^{a,b}, A. Schizzi^{a,b}, A. Zanetti^a

Kangwon National University, Chunchon, Korea

A. Kropivnitskaya, S.K. Nam

Kyungpook National University, Daegu, Korea

D.H. Kim, G.N. Kim, M.S. Kim, D.J. Kong, S. Lee, Y.D. Oh, A. Sakharov, D.C. Son

Chonbuk National University, Jeonju, Korea

J.A. Brochero Cifuentes, H. Kim, T.J. Kim, M.S. Ryu

Chonnam National University, Institute for Universe and Elementary Particles, Kwangju, Korea

S. Song

Korea University, Seoul, Korea

S. Choi, Y. Go, D. Gyun, B. Hong, M. Jo, H. Kim, Y. Kim, B. Lee, K. Lee, K.S. Lee, S. Lee, S.K. Park, Y. Roh

Seoul National University, Seoul, Korea

H.D. Yoo

University of Seoul, Seoul, Korea

M. Choi, H. Kim, J.H. Kim, J.S.H. Lee, I.C. Park, G. Ryu

Sungkyunkwan University, Suwon, Korea

Y. Choi, Y.K. Choi, J. Goh, D. Kim, E. Kwon, J. Lee, I. Yu

Vilnius University, Vilnius, Lithuania

A. Juodagalvis, J. Vaitkus

National Centre for Particle Physics, Universiti Malaya, Kuala Lumpur, Malaysia

I. Ahmed, Z.A. Ibrahim, J.R. Komaragiri, M.A.B. Md Ali³², F. Mohamad Idris³³, W.A.T. Wan Abdullah, M.N. Yusli

Centro de Investigacion y de Estudios Avanzados del IPN, Mexico City, Mexico

E. Casimiro Linares, H. Castilla-Valdez, E. De La Cruz-Burelo, I. Heredia-de La Cruz³⁴, A. Hernandez-Almada, R. Lopez-Fernandez, A. Sanchez-Hernandez

Universidad Iberoamericana, Mexico City, Mexico

S. Carrillo Moreno, F. Vazquez Valencia

Benemerita Universidad Autonoma de Puebla, Puebla, Mexico

I. Pedraza, H.A. Salazar Ibarguen

Universidad Autónoma de San Luis Potosí, San Luis Potosí, Mexico

A. Morelos Pineda

University of Auckland, Auckland, New Zealand

D. Krofcheck

University of Canterbury, Christchurch, New Zealand

P.H. Butler

National Centre for Physics, Quaid-I-Azam University, Islamabad, Pakistan

A. Ahmad, M. Ahmad, Q. Hassan, H.R. Hoorani, W.A. Khan, T. Khurshid, M. Shoaib

National Centre for Nuclear Research, Swierk, Poland

H. Bialkowska, M. Bluj, B. Boimska, T. Frueboes, M. Górski, M. Kazana, K. Nawrocki, K. Romanowska-Rybinska, M. Szleper, P. Zalewski

Institute of Experimental Physics, Faculty of Physics, University of Warsaw, Warsaw, Poland
G. Brona, K. Bunkowski, K. Doroba, A. Kalinowski, M. Konecki, J. Krolikowski, M. Misiura, M. Olszewski, M. Walczak

Laboratório de Instrumentação e Física Experimental de Partículas, Lisboa, Portugal
P. Bargassa, C. Beirão Da Cruz E Silva, A. Di Francesco, P. Faccioli, P.G. Ferreira Parracho, M. Gallinaro, N. Leonardo, L. Lloret Iglesias, F. Nguyen, J. Rodrigues Antunes, J. Seixas, O. Toldaiev, D. Vadrucio, J. Varela, P. Vischia

Joint Institute for Nuclear Research, Dubna, Russia
S. Afanasiev, P. Bunin, M. Gavrilenko, I. Golutvin, I. Gorbunov, A. Kamenev, V. Karjavin, V. Konoplyanikov, A. Lanev, A. Malakhov, V. Matveev³⁵, P. Moiseenz, V. Palichik, V. Perelygin, S. Shmatov, S. Shulha, N. Skatchkov, V. Smirnov, A. Zarubin

Petersburg Nuclear Physics Institute, Gatchina (St. Petersburg), Russia
V. Golovtsov, Y. Ivanov, V. Kim³⁶, E. Kuznetsova, P. Levchenko, V. Murzin, V. Oreshkin, I. Smirnov, V. Sulimov, L. Uvarov, S. Vavilov, A. Vorobyev

Institute for Nuclear Research, Moscow, Russia
Yu. Andreev, A. Dermenev, S. Gninenko, N. Golubev, A. Karneyeu, M. Kirsanov, N. Krasnikov, A. Pashenkov, D. Tlisov, A. Toropin

Institute for Theoretical and Experimental Physics, Moscow, Russia
V. Epshteyn, V. Gavrillov, N. Lychkovskaya, V. Popov, I. Pozdnyakov, G. Safronov, A. Spiridonov, E. Vlasov, A. Zhokin

National Research Nuclear University 'Moscow Engineering Physics Institute' (MEPhI), Moscow, Russia
A. Bylinkin

P.N. Lebedev Physical Institute, Moscow, Russia
V. Andreev, M. Azarkin³⁷, I. Dremin³⁷, M. Kirakosyan, A. Leonidov³⁷, G. Mesyats, S.V. Rusakov, A. Vinogradov

Skobeltsyn Institute of Nuclear Physics, Lomonosov Moscow State University, Moscow, Russia
A. Baskakov, A. Belyaev, E. Boos, M. Dubinin³⁸, L. Dudko, A. Ershov, A. Gribushin, V. Klyukhin, O. Kodolova, I. Lokhtin, I. Myagkov, S. Obraztsov, S. Petrushanko, V. Savrin, A. Snigirev

State Research Center of Russian Federation, Institute for High Energy Physics, Protvino, Russia
I. Azhgirey, I. Bayshev, S. Bitioukov, V. Kachanov, A. Kalinin, D. Konstantinov, V. Krychkin, V. Petrov, R. Ryutin, A. Sobol, L. Tourtchanovitch, S. Troshin, N. Tyurin, A. Uzunian, A. Volkov

University of Belgrade, Faculty of Physics and Vinca Institute of Nuclear Sciences, Belgrade, Serbia
P. Adzic³⁹, M. Ekmedzic, J. Milosevic, V. Rekovic

Centro de Investigaciones Energéticas Medioambientales y Tecnológicas (CIEMAT), Madrid, Spain
J. Alcaraz Maestre, E. Calvo, M. Cerrada, M. Chamizo Llatas, N. Colino, B. De La Cruz, A. Delgado Peris, D. Domínguez Vázquez, A. Escalante Del Valle, C. Fernandez Bedoya, J.P. Fernández Ramos, J. Flix, M.C. Fouz, P. Garcia-Abia, O. Gonzalez Lopez, S. Goy Lopez,

J.M. Hernandez, M.I. Josa, E. Navarro De Martino, A. Pérez-Calero Yzquierdo, J. Puerta Pelayo, A. Quintario Olmeda, I. Redondo, L. Romero, M.S. Soares

Universidad Autónoma de Madrid, Madrid, Spain

C. Albajar, J.F. de Trocóniz, M. Missiroli, D. Moran

Universidad de Oviedo, Oviedo, Spain

J. Cuevas, J. Fernandez Menendez, S. Folgueras, I. Gonzalez Caballero, E. Palencia Cortezon, J.M. Vizan Garcia

Instituto de Física de Cantabria (IFCA), CSIC-Universidad de Cantabria, Santander, Spain

I.J. Cabrillo, A. Calderon, J.R. Castiñeiras De Saa, P. De Castro Manzano, J. Duarte Campderros, M. Fernandez, J. Garcia-Ferrero, G. Gomez, A. Lopez Virto, J. Marco, R. Marco, C. Martinez Rivero, F. Matorras, F.J. Munoz Sanchez, J. Piedra Gomez, T. Rodrigo, A.Y. Rodríguez-Marrero, A. Ruiz-Jimeno, L. Scodellaro, I. Vila, R. Vilar Cortabitarte

CERN, European Organization for Nuclear Research, Geneva, Switzerland

D. Abbaneo, E. Auffray, G. Auzinger, M. Bachtis, P. Baillon, A.H. Ball, D. Barney, A. Benaglia, J. Bendavid, L. Benhabib, J.F. Benitez, G.M. Berruti, P. Bloch, A. Bocci, A. Bonato, C. Botta, H. Breuker, T. Camporesi, G. Cerminara, S. Colafranceschi⁴⁰, M. D'Alfonso, D. d'Enterria, A. Dabrowski, V. Daponte, A. David, M. De Gruttola, F. De Guio, A. De Roeck, S. De Visscher, E. Di Marco, M. Dobson, M. Dordevic, B. Dorney, T. du Pree, M. Dünser, N. Dupont, A. Elliott-Peisert, G. Franzoni, W. Funk, D. Gigi, K. Gill, D. Giordano, M. Girone, F. Glege, R. Guida, S. Gundacker, M. Guthoff, J. Hammer, P. Harris, J. Hegeman, V. Innocente, P. Janot, H. Kirschenmann, M.J. Kortelainen, K. Kousouris, K. Krajczar, P. Lecoq, C. Lourenço, M.T. Lucchini, N. Magini, L. Malgeri, M. Mannelli, A. Martelli, L. Masetti, F. Meijers, S. Mersi, E. Meschi, F. Moortgat, S. Morovic, M. Mulders, M.V. Nemallapudi, H. Neugebauer, S. Orfanelli⁴¹, L. Orsini, L. Pape, E. Perez, M. Peruzzi, A. Petrilli, G. Petrucciani, A. Pfeiffer, D. Piparo, A. Racz, G. Rolandi⁴², M. Rovere, M. Ruan, H. Sakulin, C. Schäfer, C. Schwick, A. Sharma, P. Silva, M. Simon, P. Sphicas⁴³, D. Spiga, J. Steggemann, B. Stieger, M. Stoye, Y. Takahashi, D. Treille, A. Triossi, A. Tsirou, G.I. Veres²⁰, N. Wardle, H.K. Wöhri, A. Zagozdinska⁴⁴, W.D. Zeuner

Paul Scherrer Institut, Villigen, Switzerland

W. Bertl, K. Deiters, W. Erdmann, R. Horisberger, Q. Ingram, H.C. Kaestli, D. Kotlinski, U. Langenegger, D. Renker, T. Rohe

Institute for Particle Physics, ETH Zurich, Zurich, Switzerland

F. Bachmair, L. Bäni, L. Bianchini, M.A. Buchmann, B. Casal, G. Dissertori, M. Dittmar, M. Donegà, P. Eller, C. Grab, C. Heidegger, D. Hits, J. Hoss, G. Kasieczka, W. Lustermaan, B. Mangano, M. Marionneau, P. Martinez Ruiz del Arbol, M. Masciovecchio, D. Meister, F. Micheli, P. Musella, F. Nessi-Tedaldi, F. Pandolfi, J. Pata, F. Pauss, L. Perrozzi, M. Quittnat, M. Rossini, A. Starodumov⁴⁵, M. Takahashi, V.R. Tavolaro, K. Theofilatos, R. Wallny

Universität Zürich, Zurich, Switzerland

T.K. Aarrestad, C. AMSler⁴⁶, L. Caminada, M.F. Canelli, V. Chiochia, A. De Cosa, C. Galloni, A. Hinzmann, T. Hreus, B. Kilminster, C. Lange, J. Ngadiuba, D. Pinna, P. Robmann, F.J. Ronga, D. Salerno, Y. Yang

National Central University, Chung-Li, Taiwan

M. Cardaci, K.H. Chen, T.H. Doan, Sh. Jain, R. Khurana, M. Konyushikhin, C.M. Kuo, W. Lin, Y.J. Lu, S.S. Yu

National Taiwan University (NTU), Taipei, Taiwan

Arun Kumar, R. Bartek, P. Chang, Y.H. Chang, Y.W. Chang, Y. Chao, K.F. Chen, P.H. Chen, C. Dietz, F. Fiori, U. Grundler, W.-S. Hou, Y. Hsiung, Y.F. Liu, R.-S. Lu, M. Miñano Moya, E. Petrakou, J.F. Tsai, Y.M. Tzeng

Chulalongkorn University, Faculty of Science, Department of Physics, Bangkok, Thailand

B. Asavapibhop, K. Kovitanggoon, G. Singh, N. Srimanobhas, N. Suwonjandee

Cukurova University, Adana, Turkey

A. Adiguzel, S. Cerci⁴⁷, Z.S. Demiroglu, C. Dozen, S. Girgis, G. Gokbulut, Y. Guler, E. Gurpinar, I. Hos, E.E. Kangal⁴⁸, A. Kayis Topaksu, G. Onengut⁴⁹, K. Ozdemir⁵⁰, S. Ozturk⁵¹, B. Tali⁴⁷, H. Topakli⁵¹, M. Vergili, C. Zorbilmez

Middle East Technical University, Physics Department, Ankara, Turkey

I.V. Akin, B. Bilin, S. Bilmis, B. Isildak⁵², G. Karapinar⁵³, M. Yalvac, M. Zeyrek

Bogazici University, Istanbul, Turkey

E.A. Albayrak⁵⁴, E. Gülmez, M. Kaya⁵⁵, O. Kaya⁵⁶, T. Yetkin⁵⁷

Istanbul Technical University, Istanbul, Turkey

K. Cankocak, S. Sen⁵⁸, F.I. Vardarli

Institute for Scintillation Materials of National Academy of Science of Ukraine, Kharkov, Ukraine

B. Grynyov

National Scientific Center, Kharkov Institute of Physics and Technology, Kharkov, Ukraine

L. Levchuk, P. Sorokin

University of Bristol, Bristol, United Kingdom

R. Aggleton, F. Ball, L. Beck, J.J. Brooke, E. Clement, D. Cussans, H. Flacher, J. Goldstein, M. Grimes, G.P. Heath, H.F. Heath, J. Jacob, L. Kreczko, C. Lucas, Z. Meng, D.M. Newbold⁵⁹, S. Paramesvaran, A. Poll, T. Sakuma, S. Seif El Nasr-storey, S. Senkin, D. Smith, V.J. Smith

Rutherford Appleton Laboratory, Didcot, United Kingdom

D. Barducci, K.W. Bell, A. Belyaev⁶⁰, C. Brew, R.M. Brown, D. Cieri, D.J.A. Cockerill, J.A. Coughlan, K. Harder, S. Harper, E. Olaiya, D. Petyt, C.H. Shepherd-Themistocleous, A. Thea, L. Thomas, I.R. Tomalin, T. Williams, W.J. Womersley, S.D. Worm

Imperial College, London, United Kingdom

M. Baber, R. Bainbridge, O. Buchmuller, A. Bundock, D. Burton, S. Casasso, M. Citron, D. Colling, L. Corpe, N. Cripps, P. Dauncey, G. Davies, A. De Wit, M. Della Negra, P. Dunne, A. Elwood, W. Ferguson, J. Fulcher, D. Futyan, G. Hall, G. Iles, M. Kenzie, R. Lane, R. Lucas⁵⁹, L. Lyons, A.-M. Magnan, S. Malik, J. Nash, A. Nikitenko⁴⁵, J. Pela, M. Pesaresi, K. Petridis, D.M. Raymond, A. Richards, A. Rose, C. Seez, A. Tapper, K. Uchida, M. Vazquez Acosta⁶¹, T. Virdee, S.C. Zenz

Brunel University, Uxbridge, United Kingdom

J.E. Cole, P.R. Hobson, A. Khan, P. Kyberd, D. Leggat, D. Leslie, I.D. Reid, P. Symonds, L. Teodorescu, M. Turner

Baylor University, Waco, USA

A. Borzou, K. Call, J. Dittmann, K. Hatakeyama, A. Kasmi, H. Liu, N. Pastika

The University of Alabama, Tuscaloosa, USA

O. Charaf, S.I. Cooper, C. Henderson, P. Rumerio

Boston University, Boston, USA

A. Avetisyan, T. Bose, C. Fantasia, D. Gastler, P. Lawson, D. Rankin, C. Richardson, J. Rohlf, J. St. John, L. Sulak, D. Zou

Brown University, Providence, USA

J. Alimena, E. Berry, S. Bhattacharya, D. Cutts, N. Dhingra, A. Ferapontov, A. Garabedian, J. Hakala, U. Heintz, E. Laird, G. Landsberg, Z. Mao, M. Narain, S. Piperov, S. Sagir, T. Sinthuprasith, R. Syarif

University of California, Davis, Davis, USA

R. Breedon, G. Breto, M. Calderon De La Barca Sanchez, S. Chauhan, M. Chertok, J. Conway, R. Conway, P.T. Cox, R. Erbacher, M. Gardner, W. Ko, R. Lander, M. Mulhearn, D. Pellett, J. Pilot, F. Ricci-Tam, S. Shalhout, J. Smith, M. Squires, D. Stolp, M. Tripathi, S. Wilbur, R. Yohay

University of California, Los Angeles, USA

R. Cousins, P. Everaerts, C. Farrell, J. Hauser, M. Ignatenko, D. Saltzberg, E. Takasugi, V. Valuev, M. Weber

University of California, Riverside, Riverside, USA

K. Burt, R. Clare, J. Ellison, J.W. Gary, G. Hanson, J. Heilman, M. Ivova PANEVA, P. Jandir, E. Kennedy, F. Lacroix, O.R. Long, A. Luthra, M. Malberti, M. Olmedo Negrete, A. Shrinivas, H. Wei, S. Wimpenny, B. R. Yates

University of California, San Diego, La Jolla, USA

J.G. Branson, G.B. Cerati, S. Cittolin, R.T. D'Agnolo, A. Holzner, R. Kelley, D. Klein, J. Letts, I. Macneill, D. Olivito, S. Padhi, M. Pieri, M. Sani, V. Sharma, S. Simon, M. Tadel, A. Vartak, S. Wasserbaech⁶², C. Welke, F. Würthwein, A. Yagil, G. Zevi Della Porta

University of California, Santa Barbara, Santa Barbara, USA

D. Barge, J. Bradmiller-Feld, C. Campagnari, A. Dishaw, V. Dutta, K. Flowers, M. Franco Sevilla, P. Geffert, C. George, F. Golf, L. Gouskos, J. Gran, J. Incandela, C. Justus, N. Mccoll, S.D. Mullin, J. Richman, D. Stuart, I. Suarez, W. To, C. West, J. Yoo

California Institute of Technology, Pasadena, USA

D. Anderson, A. Apresyan, A. Bornheim, J. Bunn, Y. Chen, J. Duarte, A. Mott, H.B. Newman, C. Pena, M. Pierini, M. Spiropulu, J.R. Vlimant, S. Xie, R.Y. Zhu

Carnegie Mellon University, Pittsburgh, USA

M.B. Andrews, V. Azzolini, A. Calamba, B. Carlson, T. Ferguson, M. Paulini, J. Russ, M. Sun, H. Vogel, I. Vorobiev

University of Colorado Boulder, Boulder, USA

J.P. Cumalat, W.T. Ford, A. Gaz, F. Jensen, A. Johnson, M. Krohn, T. Mulholland, U. Nauenberg, K. Stenson, S.R. Wagner

Cornell University, Ithaca, USA

J. Alexander, A. Chatterjee, J. Chaves, J. Chu, S. Dittmer, N. Eggert, N. Mirman, G. Nicolas Kaufman, J.R. Patterson, A. Rinkevicius, A. Ryd, L. Skinnari, L. Soffi, W. Sun, S.M. Tan, W.D. Teo, J. Thom, J. Thompson, J. Tucker, Y. Weng, P. Wittich

Fermi National Accelerator Laboratory, Batavia, USA

S. Abdullin, M. Albrow, J. Anderson, G. Apollinari, L.A.T. Bauerdick, A. Beretvas, J. Berryhill, P.C. Bhat, G. Bolla, K. Burkett, J.N. Butler, H.W.K. Cheung, F. Chlebana, S. Cihangir, V.D. Elvira, I. Fisk, J. Freeman, E. Gottschalk, L. Gray, D. Green, S. Grünendahl, O. Gutsche, J. Hanlon, D. Hare, R.M. Harris, J. Hirschauer, Z. Hu, S. Jindariani, M. Johnson, U. Joshi, A.W. Jung,

B. Klima, B. Kreis, S. Kwan[†], S. Lammel, J. Linacre, D. Lincoln, R. Lipton, T. Liu, R. Lopes De Sá, J. Lykken, K. Maeshima, J.M. Marraffino, V.I. Martinez Outschoorn, S. Maruyama, D. Mason, P. McBride, P. Merkel, K. Mishra, S. Mrenna, S. Nahn, C. Newman-Holmes, V. O'Dell, K. Pedro, O. Prokofyev, G. Rakness, E. Sexton-Kennedy, A. Soha, W.J. Spalding, L. Spiegel, L. Taylor, S. Tkaczyk, N.V. Tran, L. Uplegger, E.W. Vaandering, C. Vernieri, M. Verzocchi, R. Vidal, H.A. Weber, A. Whitbeck, F. Yang

University of Florida, Gainesville, USA

D. Acosta, P. Avery, P. Bortignon, D. Bourilkov, A. Carnes, M. Carver, D. Curry, S. Das, G.P. Di Giovanni, R.D. Field, I.K. Furic, J. Hugon, J. Konigsberg, A. Korytov, J.F. Low, P. Ma, K. Matchev, H. Mei, P. Milenovic⁶³, G. Mitselmakher, D. Rank, R. Rossin, L. Shchutska, M. Snowball, D. Sperka, N. Terentyev, J. Wang, S. Wang, J. Yelton

Florida International University, Miami, USA

S. Hewamanage, S. Linn, P. Markowitz, G. Martinez, J.L. Rodriguez

Florida State University, Tallahassee, USA

A. Ackert, J.R. Adams, T. Adams, A. Askew, J. Bochenek, B. Diamond, J. Haas, S. Hagopian, V. Hagopian, K.F. Johnson, A. Khatiwada, H. Prosper, V. Veeraraghavan, M. Weinberg

Florida Institute of Technology, Melbourne, USA

M.M. Baarmand, V. Bhopatkar, M. Hohlmann, H. Kalakhety, D. Noonan, T. Roy, F. Yumiceva

University of Illinois at Chicago (UIC), Chicago, USA

M.R. Adams, L. Apanasevich, D. Berry, R.R. Betts, I. Bucinskaite, R. Cavanaugh, O. Evdokimov, L. Gauthier, C.E. Gerber, D.J. Hofman, P. Kurt, C. O'Brien, I.D. Sandoval Gonzalez, C. Silkworth, P. Turner, N. Varelas, Z. Wu, M. Zakaria

The University of Iowa, Iowa City, USA

B. Bilki⁶⁴, W. Clarida, K. Dilsiz, S. Durgut, R.P. Gandrajula, M. Haytmyradov, V. Khristenko, J.-P. Merlo, H. Mermerkaya⁶⁵, A. Mestvirishvili, A. Moeller, J. Nachtman, H. Ogul, Y. Onel, F. Ozok⁵⁴, A. Penzo, C. Snyder, P. Tan, E. Tiras, J. Wetzel, K. Yi

Johns Hopkins University, Baltimore, USA

I. Anderson, B.A. Barnett, B. Blumenfeld, D. Fehling, L. Feng, A.V. Gritsan, P. Maksimovic, C. Martin, M. Osherson, M. Swartz, M. Xiao, Y. Xin, C. You

The University of Kansas, Lawrence, USA

P. Baringer, A. Bean, G. Benelli, C. Bruner, R.P. Kenny III, D. Majumder, M. Malek, M. Murray, S. Sanders, R. Stringer, Q. Wang

Kansas State University, Manhattan, USA

A. Ivanov, K. Kaadze, S. Khalil, M. Makouski, Y. Maravin, A. Mohammadi, L.K. Saini, N. Skhirtladze, S. Toda

Lawrence Livermore National Laboratory, Livermore, USA

D. Lange, F. Rebassoo, D. Wright

University of Maryland, College Park, USA

C. Anelli, A. Baden, O. Baron, A. Belloni, B. Calvert, S.C. Eno, C. Ferraioli, J.A. Gomez, N.J. Hadley, S. Jabeen, R.G. Kellogg, T. Kolberg, J. Kunkle, Y. Lu, A.C. Mignerey, Y.H. Shin, A. Skuja, M.B. Tonjes, S.C. Tonwar

Massachusetts Institute of Technology, Cambridge, USA

A. Apyan, R. Barbieri, A. Baty, K. Bierwagen, S. Brandt, W. Busza, I.A. Cali, Z. Demiragli,

L. Di Matteo, G. Gomez Ceballos, M. Goncharov, D. Gulhan, Y. Iiyama, G.M. Innocenti, M. Klute, D. Kovalskiy, Y.S. Lai, Y.-J. Lee, A. Levin, P.D. Luckey, A.C. Marini, C. McGinn, C. Mironov, X. Niu, C. Paus, D. Ralph, C. Roland, G. Roland, J. Salfeld-Nebgen, G.S.F. Stephans, K. Sumorok, M. Varma, D. Velicanu, J. Veverka, J. Wang, T.W. Wang, B. Wyslouch, M. Yang, V. Zhukova

University of Minnesota, Minneapolis, USA

B. Dahmes, A. Finkel, A. Gude, P. Hansen, S. Kalafut, S.C. Kao, K. Klapoetke, Y. Kubota, Z. Lesko, J. Mans, S. Nourbakhsh, N. Ruckstuhl, R. Rusack, N. Tambe, J. Turkewitz

University of Mississippi, Oxford, USA

J.G. Acosta, S. Oliveros

University of Nebraska-Lincoln, Lincoln, USA

E. Avdeeva, K. Bloom, S. Bose, D.R. Claes, A. Dominguez, C. Fangmeier, R. Gonzalez Suarez, R. Kamalieddin, J. Keller, D. Knowlton, I. Kravchenko, J. Lazo-Flores, F. Meier, J. Monroy, F. Ratnikov, J.E. Siado, G.R. Snow

State University of New York at Buffalo, Buffalo, USA

M. Alyari, J. Dolen, J. George, A. Godshalk, C. Harrington, I. Iashvili, J. Kaisen, A. Kharchilava, A. Kumar, S. Rappoccio

Northeastern University, Boston, USA

G. Alverson, E. Barberis, D. Baumgartel, M. Chasco, A. Hortiangtham, A. Massironi, D.M. Morse, D. Nash, T. Orimoto, R. Teixeira De Lima, D. Trocino, R.-J. Wang, D. Wood, J. Zhang

Northwestern University, Evanston, USA

K.A. Hahn, A. Kubik, N. Mucia, N. Odell, B. Pollack, A. Pozdnyakov, M. Schmitt, S. Stoynev, K. Sung, M. Trovato, M. Velasco

University of Notre Dame, Notre Dame, USA

A. Brinkerhoff, N. Dev, M. Hildreth, C. Jessop, D.J. Karmgard, N. Kellams, K. Lannon, S. Lynch, N. Marinelli, F. Meng, C. Mueller, Y. Musienko³⁵, T. Pearson, M. Planer, A. Reinsvold, R. Ruchti, G. Smith, S. Taroni, N. Valls, M. Wayne, M. Wolf, A. Woodard

The Ohio State University, Columbus, USA

L. Antonelli, J. Brinson, B. Bylsma, L.S. Durkin, S. Flowers, A. Hart, C. Hill, R. Hughes, W. Ji, K. Kotov, T.Y. Ling, B. Liu, W. Luo, D. Puigh, M. Rodenburg, B.L. Winer, H.W. Wulsin

Princeton University, Princeton, USA

O. Driga, P. Elmer, J. Hardenbrook, P. Hebda, S.A. Koay, P. Lujan, D. Marlow, T. Medvedeva, M. Mooney, J. Olsen, C. Palmer, P. Piroué, X. Quan, H. Saka, D. Stickland, C. Tully, J.S. Werner, A. Zuranski

University of Puerto Rico, Mayaguez, USA

S. Malik

Purdue University, West Lafayette, USA

V.E. Barnes, D. Benedetti, D. Bortoletto, L. Gutay, M.K. Jha, M. Jones, K. Jung, M. Kress, D.H. Miller, N. Neumeister, B.C. Radburn-Smith, X. Shi, I. Shipsey, D. Silvers, J. Sun, A. Svyatkovskiy, F. Wang, W. Xie, L. Xu

Purdue University Calumet, Hammond, USA

N. Parashar, J. Stupak

Rice University, Houston, USA

A. Adair, B. Akgun, Z. Chen, K.M. Ecklund, F.J.M. Geurts, M. Guilbaud, W. Li, B. Michlin, M. Northup, B.P. Padley, R. Redjimi, J. Roberts, J. Rorie, Z. Tu, J. Zabel

University of Rochester, Rochester, USA

B. Betchart, A. Bodek, P. de Barbaro, R. Demina, Y. Eshaq, T. Ferbel, M. Galanti, A. Garcia-Bellido, J. Han, A. Harel, O. Hindrichs, A. Khukhunaishvili, G. Petrillo, M. Verzetti

The Rockefeller University, New York, USA

L. Demortier

Rutgers, The State University of New Jersey, Piscataway, USA

S. Arora, A. Barker, J.P. Chou, C. Contreras-Campana, E. Contreras-Campana, D. Duggan, D. Ferencek, Y. Gershtein, R. Gray, E. Halkiadakis, D. Hidas, E. Hughes, S. Kaplan, R. Kunnawalkam Elayavalli, A. Lath, K. Nash, S. Panwalkar, M. Park, S. Salur, S. Schnetzer, D. Sheffield, S. Somalwar, R. Stone, S. Thomas, P. Thomassen, M. Walker

University of Tennessee, Knoxville, USA

M. Foerster, G. Riley, K. Rose, S. Spanier, A. York

Texas A&M University, College Station, USA

O. Bouhali⁶⁶, A. Castaneda Hernandez⁶⁶, M. Dalchenko, M. De Mattia, A. Delgado, S. Dildick, R. Eusebi, W. Flanagan, J. Gilmore, T. Kamon⁶⁷, V. Krutelyov, R. Mueller, I. Osipenko, Y. Pakhotin, R. Patel, A. Perloff, A. Rose, A. Safonov, A. Tatarinov, K.A. Ulmer²

Texas Tech University, Lubbock, USA

N. Akchurin, C. Cowden, J. Damgov, C. Dragoiu, P.R. Duder, J. Faulkner, S. Kunori, K. Lamichhane, S.W. Lee, T. Libeiro, S. Undleeb, I. Volobouev

Vanderbilt University, Nashville, USA

E. Appelt, A.G. Delannoy, S. Greene, A. Gurrola, R. Janjam, W. Johns, C. Maguire, Y. Mao, A. Melo, H. Ni, P. Sheldon, B. Snook, S. Tuo, J. Velkovska, Q. Xu

University of Virginia, Charlottesville, USA

M.W. Arenton, S. Boutle, B. Cox, B. Francis, J. Goodell, R. Hirosky, A. Ledovskoy, H. Li, C. Lin, C. Neu, E. Wolfe, J. Wood, F. Xia

Wayne State University, Detroit, USA

C. Clarke, R. Harr, P.E. Karchin, C. Kottachchi Kankanamge Don, P. Lamichhane, J. Sturdy

University of Wisconsin, Madison, USA

D.A. Belknap, D. Carlsmith, M. Cepeda, A. Christian, S. Dasu, L. Dodd, S. Duric, E. Friis, B. Gomber, R. Hall-Wilton, M. Herndon, A. Hervé, P. Klabbers, A. Lanaro, A. Levine, K. Long, R. Loveless, A. Mohapatra, I. Ojalvo, T. Perry, G.A. Pierro, G. Polese, I. Ross, T. Ruggles, T. Sarangi, A. Savin, A. Sharma, N. Smith, W.H. Smith, D. Taylor, N. Woods

†: Deceased

1: Also at Vienna University of Technology, Vienna, Austria

2: Also at CERN, European Organization for Nuclear Research, Geneva, Switzerland

3: Also at State Key Laboratory of Nuclear Physics and Technology, Peking University, Beijing, China

4: Also at Institut Pluridisciplinaire Hubert Curien, Université de Strasbourg, Université de Haute Alsace Mulhouse, CNRS/IN2P3, Strasbourg, France

5: Also at National Institute of Chemical Physics and Biophysics, Tallinn, Estonia

6: Also at Skobeltsyn Institute of Nuclear Physics, Lomonosov Moscow State University,

Moscow, Russia

- 7: Also at Universidade Estadual de Campinas, Campinas, Brazil
- 8: Also at Centre National de la Recherche Scientifique (CNRS) - IN2P3, Paris, France
- 9: Also at Laboratoire Leprince-Ringuet, Ecole Polytechnique, IN2P3-CNRS, Palaiseau, France
- 10: Also at Joint Institute for Nuclear Research, Dubna, Russia
- 11: Also at Beni-Suef University, Bani Sweif, Egypt
- 12: Now at British University in Egypt, Cairo, Egypt
- 13: Also at Ain Shams University, Cairo, Egypt
- 14: Also at Zewail City of Science and Technology, Zewail, Egypt
- 15: Also at Université de Haute Alsace, Mulhouse, France
- 16: Also at Tbilisi State University, Tbilisi, Georgia
- 17: Also at University of Hamburg, Hamburg, Germany
- 18: Also at Brandenburg University of Technology, Cottbus, Germany
- 19: Also at Institute of Nuclear Research ATOMKI, Debrecen, Hungary
- 20: Also at Eötvös Loránd University, Budapest, Hungary
- 21: Also at University of Debrecen, Debrecen, Hungary
- 22: Also at Wigner Research Centre for Physics, Budapest, Hungary
- 23: Also at University of Visva-Bharati, Santiniketan, India
- 24: Now at King Abdulaziz University, Jeddah, Saudi Arabia
- 25: Also at University of Ruhuna, Matara, Sri Lanka
- 26: Also at Isfahan University of Technology, Isfahan, Iran
- 27: Also at University of Tehran, Department of Engineering Science, Tehran, Iran
- 28: Also at Plasma Physics Research Center, Science and Research Branch, Islamic Azad University, Tehran, Iran
- 29: Also at Laboratori Nazionali di Legnaro dell'INFN, Legnaro, Italy
- 30: Also at Università degli Studi di Siena, Siena, Italy
- 31: Also at Purdue University, West Lafayette, USA
- 32: Also at International Islamic University of Malaysia, Kuala Lumpur, Malaysia
- 33: Also at Malaysian Nuclear Agency, MOSTI, Kajang, Malaysia
- 34: Also at Consejo Nacional de Ciencia y Tecnología, Mexico city, Mexico
- 35: Also at Institute for Nuclear Research, Moscow, Russia
- 36: Also at St. Petersburg State Polytechnical University, St. Petersburg, Russia
- 37: Also at National Research Nuclear University 'Moscow Engineering Physics Institute' (MEPhI), Moscow, Russia
- 38: Also at California Institute of Technology, Pasadena, USA
- 39: Also at Faculty of Physics, University of Belgrade, Belgrade, Serbia
- 40: Also at Facoltà Ingegneria, Università di Roma, Roma, Italy
- 41: Also at National Technical University of Athens, Athens, Greece
- 42: Also at Scuola Normale e Sezione dell'INFN, Pisa, Italy
- 43: Also at University of Athens, Athens, Greece
- 44: Also at Warsaw University of Technology, Institute of Electronic Systems, Warsaw, Poland
- 45: Also at Institute for Theoretical and Experimental Physics, Moscow, Russia
- 46: Also at Albert Einstein Center for Fundamental Physics, Bern, Switzerland
- 47: Also at Adiyaman University, Adiyaman, Turkey
- 48: Also at Mersin University, Mersin, Turkey
- 49: Also at Cag University, Mersin, Turkey
- 50: Also at Piri Reis University, Istanbul, Turkey
- 51: Also at Gaziosmanpasa University, Tokat, Turkey
- 52: Also at Ozyegin University, Istanbul, Turkey

- 53: Also at Izmir Institute of Technology, Izmir, Turkey
- 54: Also at Mimar Sinan University, Istanbul, Istanbul, Turkey
- 55: Also at Marmara University, Istanbul, Turkey
- 56: Also at Kafkas University, Kars, Turkey
- 57: Also at Yildiz Technical University, Istanbul, Turkey
- 58: Also at Hacettepe University, Ankara, Turkey
- 59: Also at Rutherford Appleton Laboratory, Didcot, United Kingdom
- 60: Also at School of Physics and Astronomy, University of Southampton, Southampton, United Kingdom
- 61: Also at Instituto de Astrofísica de Canarias, La Laguna, Spain
- 62: Also at Utah Valley University, Orem, USA
- 63: Also at University of Belgrade, Faculty of Physics and Vinca Institute of Nuclear Sciences, Belgrade, Serbia
- 64: Also at Argonne National Laboratory, Argonne, USA
- 65: Also at Erzincan University, Erzincan, Turkey
- 66: Also at Texas A&M University at Qatar, Doha, Qatar
- 67: Also at Kyungpook National University, Daegu, Korea